THESIS

USING A PRECISION-CUT LUNG SLICE CO-CULTURE PARADIGM TO INCREASE T-CELL POPULATIONS AND MODEL INFECTION EX VIVO

Submitted by:

Alexis T. Ehrlich

Department of Biomedical Sciences

In partial fulfillment of the requirements

For the Degree of Master of Science

Colorado State University

Fort Collins, Colorado

Summer 2024

Master's Committee:

Advisor: Stuart Tobet

Rushika Perera

Christianne Magee

ABSTRACT

USING A PRECISION-CUT LUNG SLICE CO-CULTURE PARADIGM TO INCREASE T-CELL POPULATIONS AND MODEL INFECTION EX VIVO

Precision cut lung slices (PCLS) bridge a gap between in vivo and in vitro studies by maintaining anatomical organization with structural integrity and intercellular signaling pathways. Applications of PCLS have included the modeling of inflammatory lung diseases, metabolism studies, and drug development. In the lungs, immune responses are carried out by a network of T- and B- cells, the latter of which are resident. The limited resident T-cell population of the lung diminishes accurate representations of pathogen response capacity in PCLS. Addressing this, we set out to increase pulmonary T-cell populations ex vivo. We hypothesized that thymus and bone marrow-derived T-cells would work synergistically to populate the lung in co-culture experiments. A murine organotypic lung co-culture model was developed and characterized for tissue health and T-cell recruitment over 3 days ex vivo using adult neurobasal media with 4 mM glucose + 2% B27 supplement. Lung slices were cultured independently, with bone marrow, thymus, or both. Immune colonization of the lung was assessed using immunohistochemistry for CD3+ T-cells, CD19+ B-cells and ACK2+ cells. Cells were counted in alveolar and airway spaces

after 3 days of culture. Our results demonstrate that lung co-cultured with thymus and bone significantly increased T-cell populations ex vivo, whereas lung co-cultured with thymus or bone alone did not significantly alter T-cell counts. Additionally, B-cells and C-Kit+ cell populations were not influenced by the culture paradigm. Using this paradigm, we went on to explore this lung co-culture paradigm when stimulated by an immune modulatory agent – LPS- and when an active lung infection is present using *Pseudomonas aeruginosa*. Lung and lung co-cultures had increases in T-cell counts after immune stimulation and infection. Additionally, the co-cultures further increased T-cell counts after treatment. More strikingly, the co-cultures influenced the degree of bacterial infection in the lung slices without altering the B-cell populations among cultures. Viral infections are also common pathogens that affect the lungs, so we examined then examined the ability of viral pathogens to infect precision cut lung slices. As we did not get an infection with live virus, we explored the effect of a viral mimic – Resiquimod- on lung co-cultures on the immune responses. Resiquimod and the co-cultures are both able to increase T-cell populations in lung slices ex vivo. These results suggest that the increased T-cell population corresponding with thymus and bone marrow co-culture could be a result of cell-cell interaction or the secretion of growth factors. Cell secretions or growth factor release could stimulate thymic secretion of T-cells or could stimulate T-cell proliferation in the lung, suggesting that co-culture with thymus and bone marrow can elicit a T-cell response ex vivo. T-cells are necessary for host-pathogen immune responses, most commonly by CD8+ T-cells but there are other populations of T-cells. Although there are limitations to the use of lung slices in infection studies, the results of

the co-culture and increasing T-cells is a promising step to studying pathogen response capacity in the future ex vivo.

ACKNOWLEDGEMENTS

I have received help and support from many amazing individuals over the years. First and foremost, I would like to thank my advisor Dr. Stuart Tobet for being a fantastic mentor and teacher. Working for you has been quite enjoyable and educational. You made me think harder than I have ever had to, taught me how to ask better questions, and supported me endlessly through all the modifications I made to my career path. You have provided me with tremendous opportunities and for that I am incredibly grateful.

Next, I want to thank my committee members. Dr. Perera, thank you for supporting me through all my failed experiments and helping guide me through the next steps. You made me think more critically about what aspects might be influencing the results I was observing and where that would take me. Thank you for also providing the viruses I used in my experiments and performing the plaque assays in your lab. Dr. Magee, you have made a huge difference in my life over the last few years. Thank you for providing me with a strong basis of anatomy, for providing me with a teaching opportunity and for taking the time to make sure I was adequately prepared for my oral defense. Thank you both for challenging me with concepts out of my realm of current knowledge and making me see how things are connected.

I also wanted to thank Brielle Patlin for her contributions to my thesis. Without the lung slice model, you created none of this work would have been possible. Thank you for

spending months training me how to inflate a lung and the subsequent steps for tissue culture.

For my work with *Pseudomonas Aeruginosa*, I would like to thank Dr. Brad Borlee for providing the bacteria and his student Sam Golon for streaking and dropping off the bacteria

For my work with Dengue virus and Sindbis virus, I would again like to thank Dr. Perera for providing the viruses. I would also like to thank Dr. Suad Elmegerhi for helping with sterile filtering effluents and for running the plaque assays.

I would also like to thank Dr. Luke Schwerdtfeger for his contributions to my project. Thank you for providing me with the macros used for my bacterial analysis and thank you for answering any question I asked you, no matter how dumb it was.

Next, I would like to acknowledge my laboratory support system. Hayley Templeton, working with you over the last few years has been a blessing, thank you for helping grow my interest in science and for always being a shoulder to lean on. Emily Castellanos, thank you for always brightening my days. Julietta Sheng (aka Jules), one, thank you for providing the Resiquimod I used in my experiments but also thank you for endlessly supporting me. Lastly, a big thank you to Nicholai Hagemann for helping with hours of literature review and tissue plating you endured by my side.

Thank you to everyone involved in my academic career to this point, I greatly appreciate the support and guidance you all have provided me. I look forward to utilizing

the skills I gained working in lab to my veterinary career and hope to one day be able to pay everything done for me forward to someone else.

Lastly, I would like to thank my family for their endless support, I would not be where I am today without them. Harley and Zeus, my two little King Cavalier Spaniels took on office manager positions during my time in lab. I'd like to thank them for all the work they did not put into this thesis. Thank you to Tuxie, my adorable little cat for her supervisor role, making sure I always proofread my work as she frequently edited it. Finally, thank you to my two horses, Poncho and Spirit, for all the hours of stress relief and hugs. To all - your contributions did not go unnoticed, and I am forever grateful to have you as part of my support system.

TABLE OF CONTENTS

CHAPTER 1 – INTRODUCTION

1.1 Precision cut lung slices

Precision cut lung slices (PCLS) are powerful tools to study lung physiology and an array of respiratory diseases. The use of PCLS over time has expanded immensely, originally looking at short term toxicology and metabolite production assays to currently being used to measure integrated cellular responses caused by inflammatory or infectious agents longer term (Freeman & O'Niel, 1984; Lam et al., 2023). Although generally grouped into one category, lung slices vary widely, partly due to differences in experimenter, protocol, and intended use. For instance, PCLS have been adapted for use with human lung biopsies and murine lung dissections. To obtain lung slices from either, there are protocol differences with human biopsies typically inflating the lung through larger airways in a specific lobe whereas in rodents, lung slices are inflated through the trachea. Additionally, the first generation of PCLS around the 1920's did not involve inflating the lungs, causing issues in obtaining equal sections. It was not until around the 1980's when researchers implemented the use of polymers, such as agarose, for lung inflation (Placke & Fisher, 1987; Koziol-White, 2022; Lui et al., 2019). PCLS can also differ through the media they are cultured in; some being in higher glucose solutions, others containing animal serum, and some implementing the supplementation of B27 (Viana et al., 2022; Koziol-White, 2024; Patlin et al., 2023). Despite these differences, lung slices hold several advantages over the use of immortalized cells lines or whole animals. First, slices

recapitulate native lung architecture and physiology. Like in vivo studies, lung slices maintain the airway and arterial smooth muscle contraction and ciliary beat (Li et al., 2020; Delmotte & Sanderson, 2006; Lam et al., 2023; Patlin et al., 2023; Ehrlich, unpublished observations). Lung slices contain resident cell populations that preserve their intercellular signaling pathways and replicate the cellular interactions seen in vivo. As a result, slices can be used to study cellular respiratory responses and signaling pathways between resident cell populations (Patlin et al., 2023; Lui et al., 2019, Michalaki et al., 2022). Secondly, because lung slices specifically represent lung physiology, extra-organ signaling and communication between other organ axes are eliminated, so the lung is studied in isolation. In comparison to dissociated cell cultures, slices provide complex 3D environments that replicate several aspects of lung physiology, making it a stronger model to study pathogen exposure and respiratory disease biology ex vivo.

Highlighted through the Sars-CoV-2 pandemic, respiratory pathogens can emerge rapidly, calling attention to the need for an efficient and physiologically relevant model to study respiratory disease biology. Lung slices bridge the gap between in vivo and in vitro studies, maintaining intercellular signaling pathways, recapitulating native lung physiology, and preserving the complex structure of the lung. While PCLS maintain resident immune cell populations of B-cells, natural killer cells, macrophages, dendritic cells, and some T-cells, there are some limitations to their use. Without blood or lymphatic circulation, PCLS alone are static cultures and are typically only be used to study innate immune responses as non-resident immune cells are not recruited and most studies do not implement PCLS for secondary infections. (Viana et al., 2022; Davidowich et al., 2013).

At the same time, although slices maintain immune cell populations, the lung is heterogeneous, and the populations of immune cells can vary within the lobe itself (Liu et al. 2019). Most lung slice protocols include cardiac perfusion with solutions, such as phosphate buffer solution, to remove non-resident immune cells before the lung is inflated. T-cells are typically non-resident and recruited through the circulation between peripheral lymphoid organs. The cardiac perfusions that occur before lung inflation greatly reduces the T-cell population in the lungs. Despite these limitations, PCLS have been an effective model to study respiratory disease biology.

1.2 Innate vs. Adaptive immune responses

Respiratory disease and response to infection relies heavily on innate and adaptive immune responses. The lungs directly interact with particles from the environment, most of which are filtered through the mucosal barriers in the upper airways. Physical clearance of pathogens can be achieved through coughing and sneezing. However, more virulent contaminants can be recognized by the surface epithelium, stimulating phagocytosis and activation of the immune cells through interactions with toll-like receptors (Schraufnagel, 2020; Dagenais et al., 2023; Nature immunology, 2015). Innate immunity includes the induction of anti-microbial peptides, cytokines, and chemokines. The lung epithelia, comprised of alveolar type I and II cells, is crucial for the lung's immune responses. Alveolar epithelial cells can act as antigen presenting cells for T-cells while also producing several cytokines and chemokines (Johnston et al. 2021; Debbabi et al., 2005; Lo et al., 2008; Pechkovsky et al., 2005). In addition to alveolar epithelial cells, airway epithelial cells, macrophages, monocytes, and neutrophils play primary roles in the phagocytosis of

harmful pathogens. The adaptive immune response in the lung consists of T and B-lymphocytes, antigen presenting cells, and soluble mediators. In precision cut lungs slices, unless studying secondary infections, innate immunity is the primary area of focus. Adaptive immunity usually takes 1-2 weeks to fully develop a response to new pathogens and viability of PCLS after 1 week becomes more variable, secondary infections are less likely to be studied successfully in PCLS.

While CD4+ and CD8+ T-cells play one of the largest roles in the adaptive immune response, they have roles within the innate immune response. CD4+ T-helper cells are responsible for signaling to other immune cells during infection while cytotoxic CD8+ T-cells destroy infected cells. T-cells are primed and activated in lymphoid organs, starting in the bone marrow, maturing in the thymus, and traveling to the lung and periphery once they mature. (Janeway et al., 2001; Gopalawa et al., 2023). Lymphocyte development occurs in specialized microenvironments where there are networks of nonspecialized stomal cells. The stromal cells provide signals to developing lymphocytes through secreted growth factors and cell-surface molecules, such as IL7. For T-cells, the Notch signaling pathway plays important roles in development, differentiation, and function, with Notch1 playing the most important role in T-cell maturation in the thymus (Brandstadter & Milliard, 2019). There is evidence that Notch signaling contributes to the development of B-cells in the bone marrow (Garis & Garrett-Sinha, 2021). There are numerous studies looking at the maturation of T- and B-cells, some ex vivo (Montel-Hagen et al., 2020). The basis of these studies supports the idea that lung slices could be co-cultured with similar

systems, such as bone marrow derived stromal cells, to study immunity longer term with the potential for adaptive immunity studies.

1.3 Infection

Viral and bacterial infections are becoming increasingly more prevalent, with some becoming harder to treat. Vector-borne infections, such as Dengue virus and Sindbis virus are of increasing importance. Although generally associated with more tropical climates, Dengue virus is spreading to non-equatorial climates as they become warmer. The global incidence of Dengue infections has increased from around 500 thousand cases a year in 2000 to 5.2 million cases yearly in 2019. In 2024 alone, 7.6 million cases of Dengue have been reported with 3.4 million confirmed as of April. (World Health Organization, 2024). Although not at a pandemic level, it is important to have a model to study the evolution of Dengue strains and the potential emergence of new pathogens.

The applications of PCLS have expanded overtime, more recently diving into research with infections. Some experimenters use lung slices to model viral and bacterial infectious agents and various drug therapies. Studies provide evidence that lung slices can be used to examine both viral and bacterial infections, with some instances that PCLS can have a simultaneous bacterial and viral infection (Ebsen et al., 2002). For instance, *Mycobacterium abscessus* can infect PCLS while showing similar infection rates and tissue damage to that seen in vivo (Molina-Torres et al., 2020). Studies have also been defined using primary pneumonic plague, *Pseudomonas aeruginosa,* and many bacteria that cause pneumonias, such as staphylococcus strains (Banerjee et al., 2019; Lui et al.,

2019; Viana et al., 2022; Cramer et al., 2022). At the same time, researchers are testing how viruses infect lung slices and how novel therapeutic agents might influence infections (Sewald & Donav, 2022; Michalaki et al., 2022; Rosales-Gerpe et al., 2018). The expansion of PCLS has begun to demonstrate that lung slices can be used to model infections and respiratory disease biology ex vivo.

Lower respiratory infections account for a large percentage of morbidity and mortality in children and adults worldwide. With the ability of respiratory pathogens to emerge rapidly, it is important to have an effective and efficient model to study its pathogenesis and potential drug targets. Precision cut lung slices are one model that can be used for these studies. However, the heterogenous populations of immune cells throughout the lungs limit such studies. As a result, the current study aims to increase the T-cell population in the precision cut lung slices using a co-culture paradigm with thymus and bone marrow. To study infection with co-cultures, bacterial and viral immune modulators were implemented. T-cell and B-cell responses were analyzed in a treatment and a culture paradigm dependent manner. This study examines lung-specific interactions relevant to bacterial and viral infections in the presence of T-cells.

CHAPTER 2 - USING A PRECISION-CUT LUNG SLICE CO-CULTURE PARADIGM TO INCREASE T-CELL POPULATIONS AND MODEL INFECTION EX VIVO

Graphical overview:

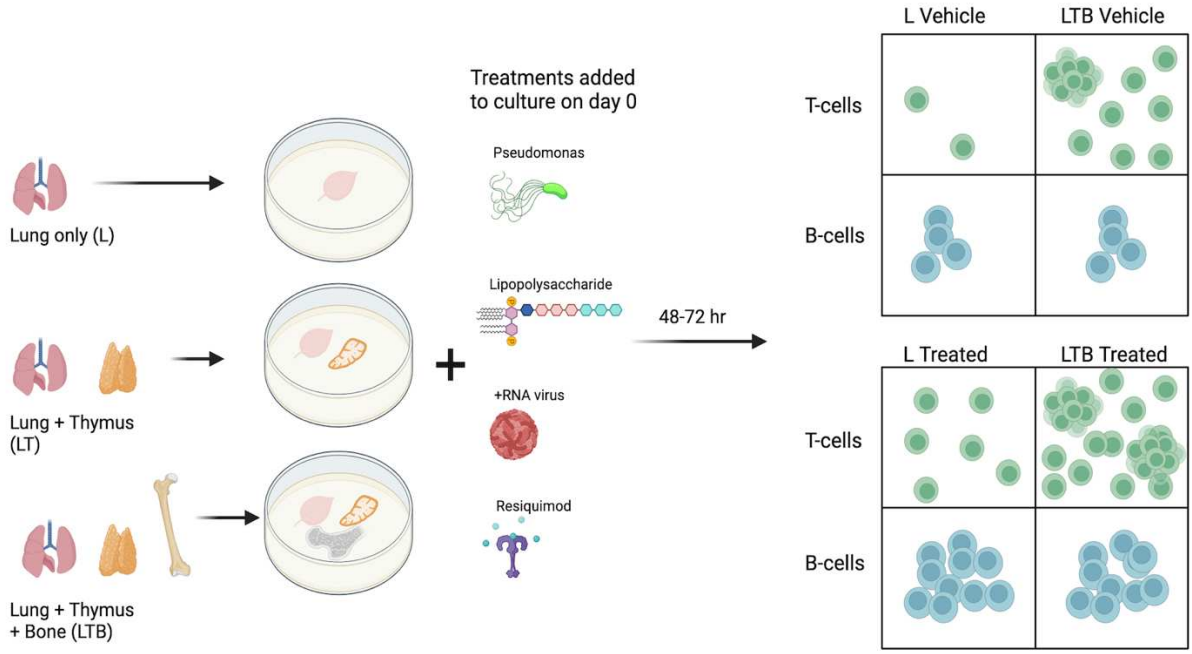

Figure 1: Graphical overview

2.1 Introduction

Bacterial and viral respiratory infections constitute a significant global health challenge due to their high prevalence and associated mortality and morbidity. Lower respiratory tract infections alone in 2019 were responsible for over 2.6 million deaths globally, making it the fourth leading cause of death overall (World Health Organization, 2020). Moreover, many bacterial pathogens are adapting antibiotic resistance, further

complicating infections and treatment options while increasing the length of hospitalizations. *Pseudomonas aeruginosa* is an opportunistic pathogen found in hospital settings and is one of the leading causes of healthcare-associated infections, particularly in intensive care units (Roulova et al., 2022). Chronic lung infections cause significant lung tissue damage and can further exacerbate other health conditions, primarily in immunocompromised populations. Studying bacterial respiratory infections is essential for preparedness in the instance of a pathogen outbreak and for understanding the mechanism in which pathogens become resistant to treatment. Having a model to examine infection, in addition to potential treatments, is vital for decreasing the public health burden these infections inflict on populations globally.

Chronic respiratory diseases and lower respiratory infections are two of the leading causes of death worldwide. Often, respiratory disease and infection cause irreversible lung damage through an imbalance of the body's inflammatory response. Currently, respiratory disease is studied with the use of live animals, in vitro cell lines, and 3D tissue cultures, some utilizing microfluidics. Precision cut lung slices (PCLS) are an organotypic lung slice model used to study a wide range of respiratory conditions, such as asthma, chronic obstructive pulmonary disease, fibrosis, and infections (Freeman & O'Niel, 1984; Lam et al., 2023). PCLS are particularly valuable in respiratory research and drug development due to their ability to mimic lung environments in vivo; maintaining cellular diversity, cell-cell interactions, and the complex 3D architecture. Moreover, lung slices maintain resident immune cell populations. While PCLS are usually static cultures and do not maintain circulation or communication with other organs, this is particularly efficacious for studying

lung biology independently, as extra humoral signaling between other organ axes is eliminated (Lui et al., 2019, Michalaki et al., 2022). Lung slices provide a unique bridge between in vivo and in vitro studies as they are more complex and realistic to native cellular composition than immortalized cell lines. PCLS have the potential to characterize respiratory interactions and signaling to a greater extent than cell lines and in a more ethically motivated paradigm to reduce animal use.

While precision cut lung slices are great models for studying respiratory disease biology, there are limitations to studying infection. PCLS maintain resident populations of B-cells, natural killer cells, macrophages, and dendritic cells. While lungs in vivo contain T-cells, ex vivo lung slices have limited T-cell populations, making studies of viral and bacterial infections challenging (Stegmayr et al., 2021; Crue et al., 2023). T-cells, particularly cytotoxic (CD8+) T-cells play crucial roles in recognizing viral antigens presented on infected cells and releasing cytotoxic molecules such as granzymes and perforin. T-helper (CD4+) cells also play a role in neutralizing viruses; however, they are involved with bacterial infections by activating macrophages and phagocytes to engulf and destroy bacteria. T-cells are responsible for releasing interferon-gamma, among other cytokines involved in the immune response to infection. When T-cells are not present in a model, such as the limited population present in PCLS, infections cannot be modeled sufficiently as that is not a native physiologic characteristic of immune cells in the lung

To enable studies of infection in a lung slice model, this study examines T-cell responses in lung co-cultures. Some studies have utilized respiratory cell lines and co-cultured them with immune cells (Alfaro-Moreno et al. 2008). Unlike lung slices, cell lines

do not recapitulate native lung physiology and co-culture with immune cells does not represent typical cell-cell interactions that would be seen in vivo. Furthermore, in vivo studies require large sample sizes to acquire replicates. Numerous precision cut lung slices can be obtained from a single animal, increasing the number of replicates in an experiment and improving statistical power while decreasing animal use. For instance, lung slices can be used to test different antimicrobials and doses to determine whether treatments are advantageous for specific pathogens, using fewer animals (Munyonho et al. 2024). However, lung slices do not recapitulate resident T-cell populations that would be seen in vivo, limiting their use in modeling infection responses. As such, this study uses lung slices co-cultured with thymus and bone marrow to increase T-cell populations in the lung and thereby study infection. The results of this study indicate that PCLS co-cultures hold significant promise for studies of viral and bacterial infections.

2.2 Methods

2.2.1 Animals

Female and male mice between 3-5 months with a C57BL/6N background were used for all experiments. Mice were multi-housed in plastic cages with aspen bedding (autoclaved Sani-chips; Harlan Teklad, Madison, WI) with a 12:12 hour light-dark cycle with ad libitum access to food (no. 2918, Envigo TD) and water. Mice were housed at Colorado State University (CSU) and cared for by Laboratory Animal Resources, an American Association for Accreditation of Laboratory Animal Care accredited (000834) unit. All animal use and procedures were approved by CSU Institutional Animal Care and Use Committee protocol #1657.

2.2.2 Generation of Lung Slices

Mice were deeply anesthetized using isoflurane and killed via decapitation. 70% EtOH was used to sterilize the abdomen and hind legs. The abdomen was opened to expose the respiratory diaphragm. The thoracic cavity was opened by puncturing through and cutting the midline of the diaphragm and then by cutting both sides of the ribs. A small cut was then made in the right atrium of the heart and animals were perfused through the left ventricle with ~37°C phosphate buffered saline (PBS) to remove non-resident immune cells. Hearts were removed and then the thymus and salivary glands were dissected away under an Olympus SZX7 dissecting scope until the trachea was visible. The thymus was placed in ice-cold Krebs buffer in (mM: 2.5 KCl, 2.5 $CaCl_2$, 126 NaCl, 1.2 $MgCl_2$, 1.2 NaH_2PO_4) for later dissection. The trachea was then slightly cut so that a ~20-gauge sterile blunted plastic needle could be inserted. The lungs were inflated using 1 ml of ~40°C 2% low melting point agarose (Gold Biotechnology, St. Louis, MO) in MQH_2O. Inflation was achieved when the lung was visibly full on the edge of each lobe but not to the point where there would be a rupture. The needle was removed, and tweezers were used to grab and hold the trachea so no agarose would flow out. Lungs were removed and immediately placed in ice-cold Krebs buffer. Using the Olympus SZX7 dissecting scope, the lobes were separated from the trachea and connecting airways. Each lobe was then blocked with ~40°C 8% low melting point agarose in MQH_2O at 4°C for 4 minutes to permit the agarose to polymerize. Using a vibrating microtome (VT1000S; Leica Microsystems, Wetzlar, Germany), 250 µm slices of lung were taken and collected into 5 mL of 4°C Hibernate (Life Technologies, Grand Island, NY) in 60 mm dishes (Corning, Corning, NY). Slices were in

Hibernate for at least 15 minutes and a maximum of 2 hours. After, the Hibernate media was removed and replaced with 5 mL of homemade 4 mM glucose CTS with 2% B27 supplement (Life Technologies) for 35 minutes at 37°C to permit slices to regain physiological temperature. Slices were plated onto 35 mm plastic bottom culture dishes (Corning and Corning Falcon, Corning, NY) without media for 15 minutes at 37°C and 100% humidity to promote adherence to the dish. Slices were then covered with 40 µL of collagen solution (vol/vol: 10.4% 10× MEM, 1.9% PS, 4.2% sodium bicarbonate, and 83.5% collagen (PureCol; Inamed, Fremond, CA)) for 10 minutes at 37°C before adding 0.8 ml of 4 mM glucose CTS media with 2% B27 supplement to each dish. An air-liquid interface was created using 0.8 mL of media for the culture. Media was changed daily until slices were killed. It is important to note that the media was serum-free to increase reproducibility of experiments (Schwerdtfeger et al. 2019). In addition, no antibiotics were used in the culture media to maintain the natural microbiome found in the lung, maintaining the translational relevance of these lung slices.

2.2.3 Generation of Thymus Slices

During the generation of lung slices, the thymus is placed in ice-cold Krebs buffer. The thymus was cleaned of any remaining mediastinal fat and salivary glands. Tweezers were used to gently lift the thymus out of Krebs, without grabbing or pinching, and then the thymus was dabbed on a sterile Kimwipe to remove excess buffer. The thymus was blocked and sliced in the same manner described above. As the thymus has a butterfly appearance, slices were obtained by turning the butterfly on its side and cutting horizontally; this allowed for more sections to be collected.

2.2.4 Bone Dissection

Prior to taking lung and thymus slices, 70% EtOH was used to clean the fur to decrease the risk of infection in the culture. The bony prominence (ischiatic tuberosity) of the pelvis was located and palpated bilaterally. Both legs were cut at the coxofemoral joint, maintaining the head of the femur on each bone. A small cut was made in the distal crus and the skin was reflected and cut near the calcaneus bone. Legs were then placed in 1X Krebs buffer and dissected using an Olympus SZX7 scope. Musculature, tendons, and cartilaginous tissue were removed. The femur and tibia were then bluntly cut into ~2 mm (about 0.08 in) pieces and placed in 5 mL of cold Hibernate at 4°C for 15 minutes. Hibernate was removed and replaced with 5 mL of homemade 4 mM glucose CTS with 2% B27 supplement (Life Technologies; 17504044) at 37°C to permit slices to regain physiological temperature for at least 35 minutes. Bone pieces were added to cultures after the lung and thymus were plated and covered with collagen overlay. Bone was not covered with overlay and was just placed in the media near the organ slices.

2.2.5 Generation of Spleen Slices

The lung and thymus were removed before obtaining the spleen. The abdominal cavity was opened while visualizing the respiratory diaphragm to enter the thoracic cavity. The spleen was then visualized, the gastrosplenic ligament was cut and the greater omentum was removed. The spleen was placed in ice-cold 1X Krebs and then under the Olympus SZX7 dissecting scope the remaining mesentery was removed. Slices were blocked and sectioned as described above. Spleens were sliced width wise.

2.2.6 Plating of Co-Cultures

Tissue slices were plated in 35mm plastic bottom culture dishes as follows: lung (L), lung + thymus (LT), lung + thymus + bone (LTB), lung + spleen (LS), and lung + bone (LB). Each organ slice received 40 µL of collagen overlay. All dishes received 0.8 mL of 4 mM glucose CTS media + 2% B27 supplement regardless of how many tissue slices were in each dish to maintain the air-liquid interface. The bone was the only element of the culture that was not overlayed in collagen and that was not exactly 250 µm in width. The tissues were plated close together (within 1 mm) but without contact (Supplemental Figure 1A).

2.2.7 *Pseudomonas aeruginosa (P.Aeruginosa)*

P. aeruginosa (Dr. Brad Borlee, CSU)-conjugated to green fluorescent protein (PAP2-eGFP) was streaked onto an agar plate and incubated overnight to isolate single colonies. A flame sterilized loop was used to take single colonies and place them in 1 mL of lysogeny broth to make bacterial stocks. Stocks were incubated overnight at 37°C and then were frozen at -80°C until use. Before use, stocks were thawed in the incubator at 37°C for 4-6 hours for the bacteria to enter its exponential growth phase. A serial dilution of the stock was then made. For all experiments, a 1:1,000,000 dilution was deemed appropriate for lung slice experiments. Each culture dish received 10 µL of diluted bacteria into 0.79 mL media. At this concentration, there was no overgrowth of bacteria. After 24 hours in culture, infected media was replaced with 0.8 mL.

2.2.8 Dengue and Sindbis virus

Dengue and Sindbis viral stocks were grown in the Perera laboratory according to standard techniques (St. Clair et al., 2022; Jose et al., 2012). Briefly, the protocol is as follows: viral RNA transcribed from cDNA clone was transfected. 5-7 days post infection,

plaques were collected into 1X PBS and incubated at 4°C until the virus was released into the PBS. T25 of c6/36 cells were infected with the plaque and incubated for 1-2 hours for the cells to uptake the virus. The inoculum was then removed, and cells were overlayed with 5 mL modified eagle's medium (MEM) (+ 2% FCS + 25mM HEPES) and incubated for 4-7 days. Viral supernatant was collected, and cell debris was spun down, aliquots made, and supernatant saved. Using baby hamster kidney cells, a titer of the P1 viral supernatant was then made. To amplify and make P2, P3, and P4 viral stocks, 1xT150 of C6/36 cells were used. Media was removed from cells and cells were washed with 1X PBS. Cells were infected with 0.25-0.5 mL of P1-P3 stock at a MOI of 0.01-0.1 and supplemented with 5 mL MEM (+ 2% FCS + 25mM HEPES) and incubated for 2 hours at room temperature on a rocker. 60 mL MEM (+ 2% FCS + 25mM HEPES) was then added. Cells were then incubated at 30°C for 7-10 days until there were signs of cell detachment. Supernatant was harvested and placed into a 50 mL falcon tube and centrifuged at 1000xg for 5 minutes to remove cell debris. Supernatant was removed and aliquots made. Aliquots were then stored at -80°C until use.

Dengue stocks used for the experiments had a concentration of 1.3×10^8 PFU/mL. Additionally, Sindbis stocks used for the experiments had a concentration of 3.0×10^7 PFU/mL. Further experiments used dengue virus grown in 4 mM glucose CTS media + 2% B27 supplement that had a concentration of 4.2×10^7 PFU/mL. Dengue virus grown in 25 mM glucose CTS neurobasal media (Gibco, Thermofisher, NY) had a concentration of 3.7×10^7 PFU/mL. All viruses were collected on passage day 5. The lower glucose media grew faster, so it was collected on day 7, whereas the higher one grew slower and was collected

on day 8. Stocks were placed in the –80 °C freezer until use. Viral stocks were thawed in the incubator for 4 hours before being added to the lung cultures at concentrations of 10 µL, 50 µL, 100 µL, and 800 µL of virus per 0.8 mL of media.

2.2.9 Resiquimod

Resiquimod (HY-13740, MedChemExpress) was reconstituted in phosphate buffered saline solution at 1 mg/mL. Studies using Resiquimod in vivo have published doses at 2 mg/kg of body weight (Sheng and Tobet, 2024) and in vitro doses range from 5-2000 µg/mL (Anfray et al., 2021; Zhang et al., 2023).10 µL of Resiquimod stock was added to 0.790 mL of media- making the final concentration added 12.5 µg/mL.

2.2.10 Treatments added to culture

Table 1: Culture Treatment Overview

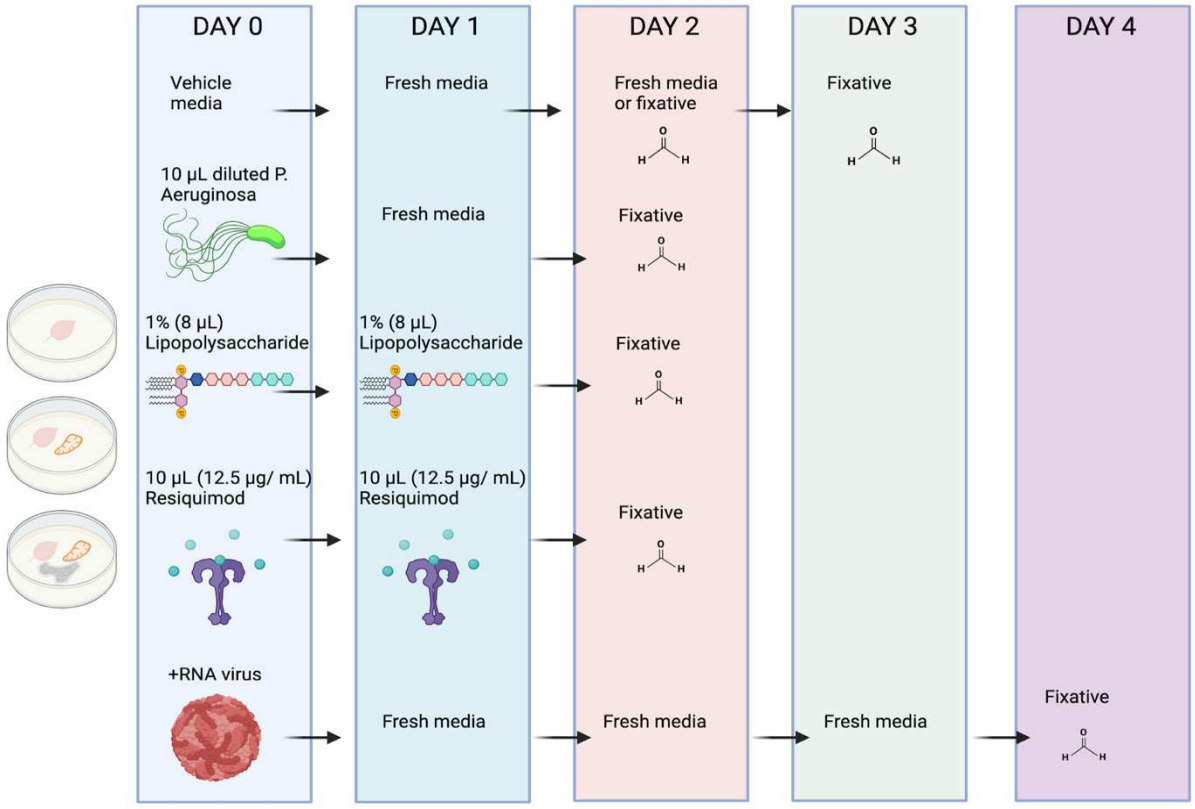

- Bacterial experiments: Slices were administered treatments at 0 hours. Slices either received no treatment (vehicle media), 1% lipopolysaccharide (LPS), or 10 µL *P. Aeruginosa*. Stock concentration of LPS was 1 mg/ml. Media was changed every 24 hours. At that time, only LPS treated dishes continued to receive 1% LPS in the media. Pseudomonas treated tissue and vehicles received regular media for the remaining days of culture. Tissue was killed 4% paraformaldehyde fixative after 48 hours of ex vivo culture.
- Viral experiments: Slices either received no treatment (vehicle media), Dengue or Sindbis virus, or 10 µL Resiquimod. Media was changed every 24 hours. At that time, only Resiquimod treated dishes continued to receive Resiquimod in the media. Vehicles, virus infected, and mock virus treated tissue received regular media for the remaining days of culture. Tissue was killed with 4% paraformaldehyde after 48 hours. Resiquimod (R-848): The TLR7/8 agonist was added to dishes at a concentration between published in vivo and in vitro doses. 10 µL of Resiquimod was added to 0.79 mL media. Every 24 hours, this dose was readministered along with the addition of fresh media.

2.2.11 Immunohistochemistry

Tissue slices were fixed with 4% paraformaldehyde at room temperature for 15 minutes and then washed 3 times with room temperature 0.05M phosphate buffer solution (PBS; pH 7.4) in 5-minute intervals. Slices were then incubated in sodium borohydride at 4°C for 2 hours and subsequently rinsed with PBS 3 times at 5-minute intervals. They were incubated in a blocking solution comprised of PBS with 5% normal goat serum (NGS;

Lampire Biological, Pipersville, PA), 0.3% Triton X (Tx), and 3% hydrogen peroxide for 1 hour. After, the tissue was placed in an additional block with a fresh change of hydrogen peroxide for 1 hour. The tissue was then placed in primary antibody made with antisera (PBS, 5% NGS, and 0.3% Tx). Tissue was then incubated in a primary antisera (see Table 1) solution containing 5% NGS, 0.3% TX, and primary antibodies (CD3, CD19, and ACK2 at a concentration of 2 µg/mL) for 5 days at 4°C. Chicken anti-green-fluorescent-protein was run 1:1000. Sindbis nucleocapsid protein was run at 1:500 and the Dengue E-protein was run at 2000 µg/mL.

Table 2: Immunohistochemistry antibodies

Primary Antibodies	**Source**	**Secondary Antibodies**	**Source**	**Tertiary Antibodies**	**Source**	**Marker for:**
CD3	Ab5690 abcam	Biotin-SP conjugated anti-rabbit	711-065-152 Jackson ImmunoResearch	Streptavidin Alexa Fluor 594	S32356 Invitrogen	T-cells
CD19	14-0199-82 eBioscience	Alexa Fluor 488 goat anti-rat	A11006 Invitrogen	---	---	B-cells
ACK2	NBP1-43359 Novus Biologicals	Alexa Fluor 594 goat anti-rat	A11007 Invitrogen	---	---	CD117/c-kit Hematopoietic stem cells, mast cells
GFP	Ab16901 Chemicon International	Alexa Fluor 488 goat anti-chicken	A11039 Invitrogen	---	---	Tagged pseudomonas aeruginosa
DENV-2	NBP2-52666 Novus Biologicals	Biotin-SP conjugated anti-rabbit	711-065-152 Jackson ImmunoResearch	Streptavidin Alexa Fluor 647	S32364 Invitrogen	Dengue Virus type 2 antigens.
Sindbis	Sindbis nucleocapsid protein Not commercially available	Alexa Fluor 488 goat anti-rabbit	A11008 Invitrogen	---	---	Sindbis

After 5 days, primary antisera were removed, and tissue was washed with cold PBS with 1% NGS and 0.02% Tx at 4°C 4 times in 30-minute intervals per wash. Fluorescent and

biotin conjugated secondaries (see Table 1) were then made with PBS, 1% NGS and 0.32% Tx and incubated for 24 hours at 4°C. Secondary antisera were made using BT anti-rabbit (1:2500; 0.44 µg/mL), AF 594/488 anti-rat (1:500; 4 µg/mL), AF 488 anti-chicken (1:500; 4 µg/mL), and AF 488 anti-rabbit (1:500; 4 µg/mL) . After 24 hours, the secondaries were removed, and the tissue was washed with PBS plus 0.02% Tx four times at 30-minute intervals at room temperature. Tertiary reagents were then made with a 0.32% Tx PBS solution and incubated for three hours. Alexa Fluor 594 and conjugated to streptavidin and Alexa Fluor 488 streptavidin were used at a concentration of 1:500 or 4 µg/mL and incubated for 3 hours. After 3 hours, the tissue was washed with room temperature PBS at 30-minute intervals for 4 changes. The tissue was then mounted on subbed slides and cover-slipped with Aqua-Poly/Mount (Polysciences, Warrington, PA).

2.2.12 Imaging and statistical analysis

Images were obtained using an Olympus BX61WI epifluorescent scope with a Hamamatsu C11440 ORCA Flash camera. Z-stacks were taken at 0.5 µm intervals, 20 µm above and below the tissue center. Z-stacks of 3 airways and 3 alveolar spaces were obtained for CD3+ cell analysis. CD19+ cells were counted throughout the entire slice. Images were imported into Olympus cellSens software where they were processed for contrast and optical thresholds to identify cellular elements. CD3+ cell populations were counted in airway and alveolar space ROIs. Importantly, for CD3+ cells, analysis of all the airways in each slice tissue yielded similar results compared to counting all the cells in the slice. Cells were counted by hand and confirmed by an individual blinded to treatment and culture paradigm. Cell counts were loaded into GraphPad Prism 10.2.3 to analyze culture

paradigms and lung regions. A two-way ANOVA was run with a Tukey post hoc test, and relative plots created. All data is presented +/- standard error of the mean and $p < 0.05$* was considered statistically significant, $P < 0.01$**, and $p < 0.001$***.

For *P. Aeruginosa* infected, LPS treated, or Resiquimod treated tissue, both females and males were used. Data from both sexes was combined and a two-way ANOVA was run by region (airway or alveolar) and for culture paradigm with control and treated tissue (alveolar/airway x vehicle/(LPS/ *P. Aeruginosa* /Resiquimod) for immune cells. A Tukey post hoc analysis was run, and relative graphs were made. All data is presented +/- standard error of the mean and $p < 0.05$* was considered statistically significant, $P < 0.01$**, and $p < 0.001$***.

P. Aeruginosa infected tissue was imaged using an Olympus BX61WI epifluorescent microscope with a Hamamatsu C11440 ORCA Flash camera. Z-stacks were taken at 0.5 µm intervals 20 µm above and below the center of the tissue. Z-stacks were then converted to max-projections and 2D deconvoluted using Olympus' Cell Sens software. Images were exported as ORI files (Olympus raw images) and imported into NIH FIJI. Images were then contrasted, thresholded, and eroded. The bacterial particles were then analyzed for percent area in the selected ROI's (alveolar vs airway). As there were no sex differences noted in the data, the data were combined by sex for subsequent analyses. Measurements were then put into GraphPad Prism and a two-way ANOVA was run comparing culture paradigm and *P. Aeruginosa* infection in the airway or alveolar space. A Tukey post hoc test was run, and relative graphs were made. All data is presented +/- standard error of the mean and $p < 0.05$* was considered statistically significant, $P < 0.01$**, and $p < 0.001$***.

2.2.13 Plaque assays

Plaque assays were done in the Perera lab by Dr. Suad Elmegerhi according to a standard protocol. Briefly, ~80% confluence baby hamster kidney (BHK) cells in 6-well plates were used. 10-fold dilutions of the virus were made: 270 µL PBS (+ Ca++, Mg++) + 1% FBS were put into each tube used for the dilution. The first tube received 30 µL of the concentrated effluent collected from the lung slice experiments. The tube was then vortexed and 30 µL of solution was added to the next tube and repeated until the dilution desired was achieved. With the BHK cells, the media was removed, and the cells were washed with 1X PBS. PBS was then removed. 250 µL of each viral dilution was added to each well. Plates were then placed on a rocker and incubated at room temperature for 1-2 hours. 3 mL overlay, with a final concentration of 1X MEM, 5% fetal bovine serum (FBS), 1% agarose was added to each well and gently swirled. Cells were then incubated at 37°C for 6 days. After 2 days of culture, 1 mL MEM + 10% FCS was added to prevent the agarose and cells from drying out. After the 6 days, plaques were stained with 2 ml/well of Neutral Red solution (1 mL NRS + 11 mL PBS) and incubated overnight at 37°C. Plaques were then counted. PFU/mL = plaque number x dilution factor x 4.

2.3 Results

2.3.1 Lung slices can be infected with *Pseudomonas aeruginosa*

Treatment of lung slices with a green fluorescent protein tagged *P. Aeruginosa* strain indicated that slices could be infected ex vivo. When lung slices were infected with *P. Aeruginosa* resident CD19+ B-cell populations significantly expanded ($P = <0.0001$) while T-cells increased non-significantly ($P = 0.1039, 0.115$; airway, alveolar). Moreover, it

was found that lung slices contained limited numbers T-cells. 250 μm slices contain an average of 11.0 T-cells near each large airway. As T-cells are vital for immune signaling during infection, it is important to maintain a population of T- cells in PCLS to study pathogen exposure ex vivo.

2.3.2 Lung slices co-cultured with immune organs

To determine if immune cells could be expanded in lung slices ex vivo, cultures using thymus, thymus and bone, and bone were generated (Figure 2). Resident T-cell populations, albeit small and transitory, tend to cluster near airways. After 72 h in culture, CD3+ T-cell populations were significantly increased dependent on culture paradigm ($P < 0.0001$, $n = 5$) but the increases were not regionally dependent ($P = 0.8648$, $n = 5$). When the lung was cultured with thymus (Figure 2B; $P = 0.8778$), cultured with bone (Figure 2D; $P = 0.9100$), or cultured with spleen (Figure 2C; $P=0.4253$), T-cells did not significantly increase in the airway. Strikingly, when lung slices were cultured with bone and thymus together, T-cell populations significantly increased by 348.7% (Figure. 2E; $P = 0.0047$, $n = 5$) in the airway.

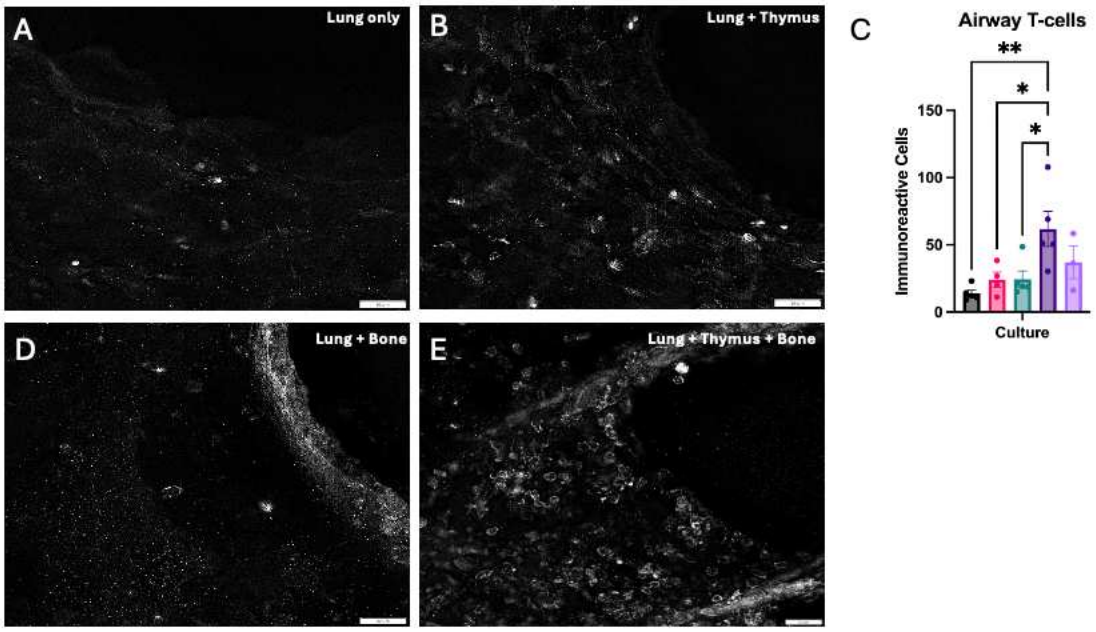

Figure 2: T-cells in the airways of lung slices. Culture of lung slices with thymus, bone, or thymus and bone resulted in differences in T-cell populations among cultures. Lung slices cultured independently have very few T-cells near the airway (A). There were no significant differences in T-cell counts in lung cultured with thymus (B) or lung cultured with bone (D). When lung was cultured with thymus and bone, there was a significant T-cell increase in the lung (E). Average number of T-cells with each culture is represented in the graph (C). The black bar represents lung cultured independently (n=5), pink represents lung with bone (n=4), teal represents lung with thymus (n=5), dark purple represents lung with thymus and bone (n=5), and light purple represents lung with spleen (n=3). Scale bars are 20 μm.

T-cells were then assessed in the alveolar space. When the lung was cultured with thymus (Figure 3B; P = 0.7168), cultured with bone (Figure 3D; P = 0.9950), or cultured with spleen (Figure 3C; P = 0.3801), T-cells did not significantly increase in the alveolar space. Strikingly, when lung slices were cultured with bone and thymus together, T-cell populations significantly increased by 376.7% (Figure 3E; P = 0.0247, n = 5) in the alveolar space.

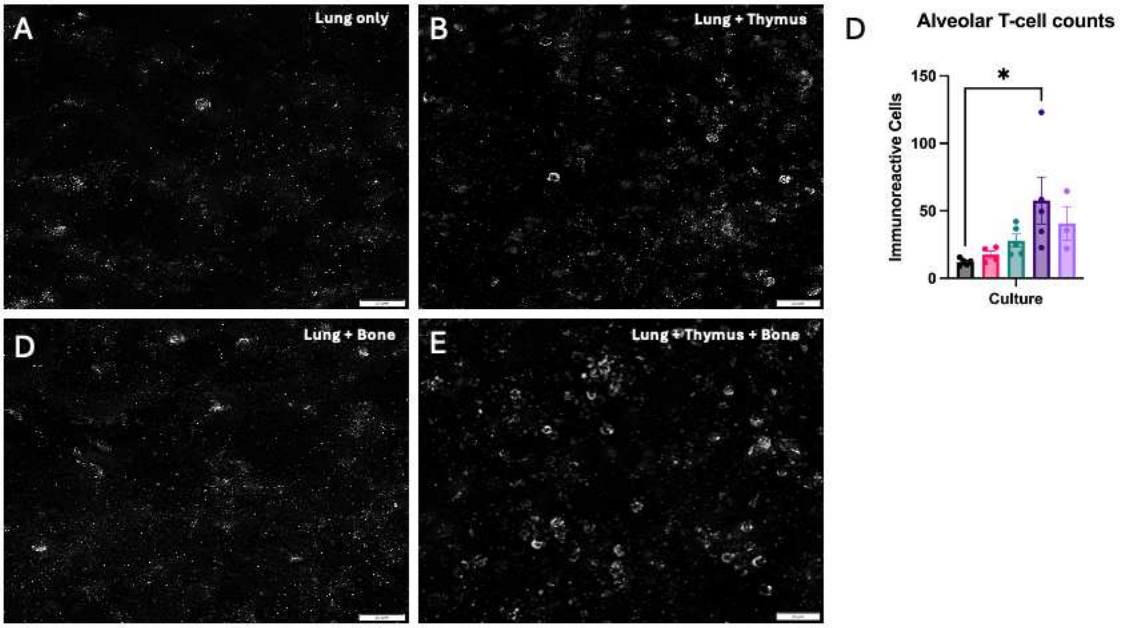

Figure 3: T-cells in the alveoli of lung slices. Culture of lung slices with thymus, bone, or thymus and bone resulted in differences in T-cell populations among cultures. Lung slices cultured independently have very few T-cells in the alveolar space(A). There were no significant differences in T-cell counts in lung cultured with thymus (B) or lung cultured with bone (D). When lung was cultured with thymus and bone, there was a significant T-cell increase in the lung (E). Average number of T-cells with each culture is represented in the graph (C). The black bar represents lung cultured independently (n=5), pink represents lung with bone (n=4), teal represents lung with thymus (n=5), dark purple represents lung with thymus and bone (n=5), and light purple represents lung with spleen (n=3). Scale bars are 20 μm.

With the apparent T-cell response in co-culture, it was important to look at other immune cell populations. Hematopoietic stem cells and mast cells were labeled for ACK2 immunoreactive cells. ACK2+ cells did not vary in number between culture paradigms ($P = 0.5653$) or by anatomical regions in the lung cultures ($P = 0.6042$) (Supplemental Figure 2). Additionally, B-cells (labeled with CD19 did not vary among culture paradigms ($P = 0.8999$) (Supplemental Figure 3). CD19+ cells were counted on both day 2 and day 3 of culture. After both 48 h and 72 h in culture, CD19+ B-cells did not vary between culture paradigm ($P = 0.6527$; $n = 3$ (72 h) vs $n = 6$ (48 h)) or day ($P = 0.5710$).

2.3.3 Co-cultures and *P. Aeruginosa* infection: T-cell's

When the co-cultures were originally tested, slices were co-cultured for 72 hours. In the infection experiments, slices were cultured for 48 hours. T-cell counts did not statistically differ between timepoints. For these experiments, lipopolysaccharide (LPS), an endotoxin released from the outer membrane of gram-negative bacteria, was used to mimic bacterial infection. Additionally, tissue was infected with a green fluorescent *Pseudomonas aeruginosa* strain (PA-eGFP). As we saw in previous experiments, lung can have increased T-cell populations as a result of co-culture with thymus and bone ($P < 0.0001$). This trend was repeated with an additional 6 animals. Similarly, T-cells after 48 hours lung co-culture with thymus and bone increased by 382.9% (Figure 4; $P < 0.0001$) in the airway and by 432.5% (Fig 5; $P < 0.0001$) in the alveolar space.

When the cultures were treated with 1% LPS, an immune modulator, T-cells increased by treatment and culture paradigm. Lung co-cultured with thymus and treated with LPS had non-significant increases in T-cell counts in both the airway ($P = 0.1857$) and in the alveolar space ($P = 0.1853$) compared to lung treated with LPS. Furthermore, when lung co-cultures with thymus and bone were treated with LPS, T-cells significantly increased by 204.6% (Figure 4F; $P < 0.0001$) in the airway and by 245.4% (Figure 5F; $P < 0.0001$) in the alveolar space when compared to LPS lung cultured independently. When LPS co-cultures were compared to their vehicle controls, lung cultured independently (Figure 4A/B, 5A/B; $P = 0.1793, 0.1589$; airway, alveolar) did not have significant increases in T-cell counts. However, LPS lung with thymus co-culture had an increase in T-cells by 99.3% ($P = 0.0534$) in the airway and by 133.7% ($P = 0.0248$) in the alveolar space, as

compared to its vehicle control. Furthermore, with LPS lung cultured with thymus and bone, T-cells increased by 56.8% (Figure 4E/F; P = 0.0048) in the airway and by 76.6% (Figure 5E/F; P = 0.0002) in the alveolar space, as compared to its vehicle control.

As *P. Aeruginosa* is a gram-negative pathogen, LPS is a component of its outer membrane. Unsurprisingly, we saw similar results with administered LPS and *P. Aeruginosa* infection. Similarly, when lung was cultured independently and infected with *P. Aeruginosa,* T-cell counts did not significantly increase when compared to the vehicle lung culture in either the airway (Figure 4A/C) or the alveolar space (Figure 5A/C). When lung was cultured with thymus and infected with *P. Aeruginosa*, T-cells did not significantly increase in the airway or alveolar space compared to lung infected with *P. Aeruginosa*. With lung slices co-cultured with thymus and bone marrow and infected with *P. Aeruginosa*, T-cells increased by 204.4% (Figure 4E/G; P < 0.0001) in the airway and by 201.1% (Figure 5E/G; P = <0.0001) in the alveolar space. With *P. Aeruginosa* infected lung cultured with thymus, T-cells increased by 97.5% (P = 0.0587) in the airway and by 102.4% (P = 0.0285) in the alveolar space, as compared its vehicle control. Furthermore, with *P. Aeruginosa* infected lung cultured with thymus and bone, T-cells increased by 71.3% (P = 0.0004) in the airway and by 62.9% (P = 0.0019) in the alveolar space, as compared to vehicle control.

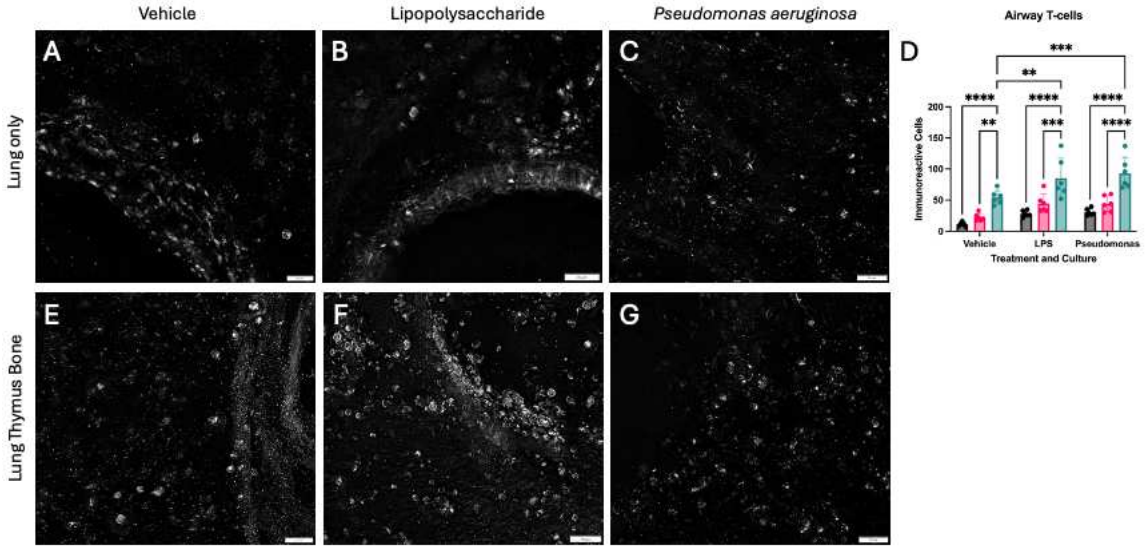

Figure 4: Airway T-cells after treatment. Vehicle lung slices (A) had non-significant T-cell increases with LPS (B) and *P. aeruginosa* (C). Vehicle lung with thymus and bone (E) had significant increases in T-cells with LPS (F) and *P. aeruginosa* (G). There were no significant differences in T-cell increases between LPS and *P. aeruginosa* for either group. Average number of T-cells with each culture is represented in the graph (D). The black bar represents lung cultured independently, pink represents lung with thymus, teal represents lung with thymus and bone. Scale bars are 20 μm.

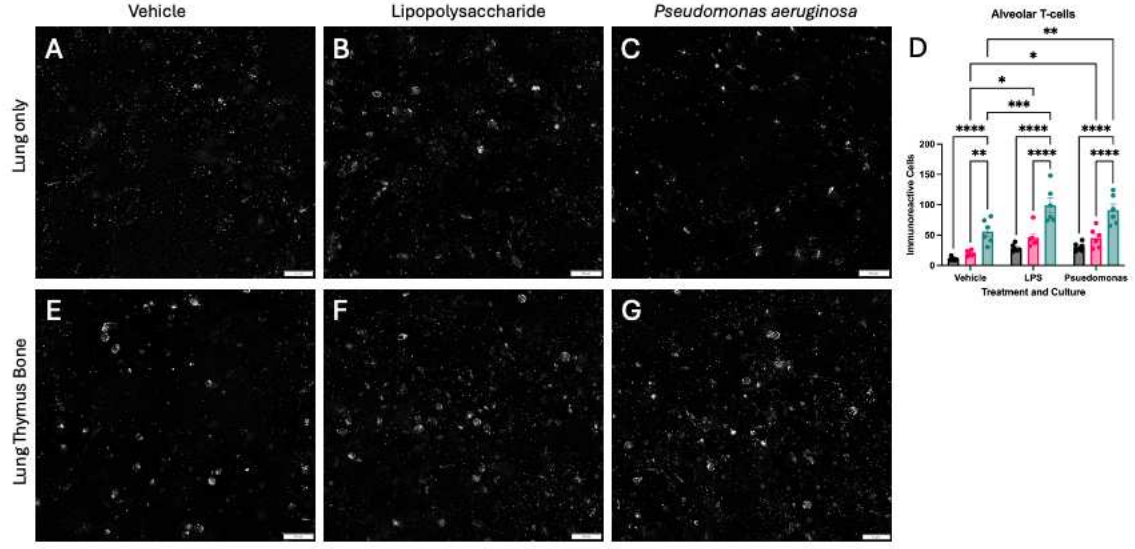

Figure 5: Alveolar T-cells after treatment. Vehicle lung slices (A) had non-significant T-cell increases with LPS (B) and *P. aeruginosa* (C). Vehicle lung with thymus and bone (E) had significant increases in T-cells with LPS (F) and *P. aeruginosa* (G). There were no significant differences in T-cell increases between LPS and *P. aeruginosa* for either group. Average number of T-cells with each culture is represented in the graph (D). The black bar represents lung cultured independently, pink represents lung with thymus, teal represents lung with thymus and bone. Scale bars are 20 μm.

2.3.4 Co-cultures and *P. Aeruginosa* infection: B-cell's

As seen previously, B-cells do not increase as a result of culture paradigm ($P = 0.1922$). However, exposure to exogenous LPS or infection with *P. Aeruginosa* significantly increased the B-cell populations to equal levels across culture groups (Supplemental Figure 4; $P < 0.0001$). *P. Aeruginosa* infected tissue vs LPS treated tissue showed similar increases in B-cells but there was no significant difference between treatments. Interestingly, B-cell populations slightly decreased with co-cultures compared to the lung cultured independently. This was a similar trend with co-cultures treated with LPS or infected with *P. Aeruginosa*. However, these decreases were not statistically significant.

When lung slices were cultured independently and treated with LPS, B-cells increased by 117.9% ($P < 0.0001$), compared to its vehicle control. When lung slices cultured independently were infected with *P. Aeruginosa*, B-cells increased by 153.1% ($P < 0.0001$), compared to its vehicle control. Comparing lung cultured independently with treatment – LPS or *P. Aeruginosa* – there was no significant difference between the B-cell increases observed between treatments ($P = 0.3562$). When lung slices were cultured with thymus and treated with LPS, B-cells increased by 108.4% ($P = 0.0008$) as compared to its

vehicle control. When the lung and thymus co-culture was infected with *P. Aeruginosa*, B-cells increased by 167.6% ($P < 0.0001$), compared to its vehicle control. Similarly, when lung slices were cultured with thymus and bone and treated with LPS, B-cells increased by 101.1% ($P = 0.0011$) when compared to its vehicle control. When lung was co-cultured with thymus and bone and infected with *P. Aeruginosa*, B-cells increased by 110.1% ($P = 0.0004$) when compared to vehicle control.

3.3.3 *P. Aeruginosa* infection and co-culture

Using the co-culture method where T-cells are then present it was observed that *Pseudomonas* aeruginosa infection was decreased due to culture ($P = <0.0001$), with no differences between region: airway vs alveolar ($P = 0.7821$). When lung was cultured with thymus there was no significant decrease in *P. Aeruginosa* infection; infection in the airway decreased non-significantly by 6.8% (Figure 6B; $P = 0.9467$) in the airway and by 40.0% (Figure 6F; $P = 0.0522$) in the alveolar space. In comparison to lung cultured independently, *P. Aeruginosa* infection in lung cultured with thymus and bone was significantly reduced by 69.1% (Fig 6C; $P = 0.0089$) in the airway and 82.5% (Fig 6G; $P < 0.0001$) in the alveolar space.

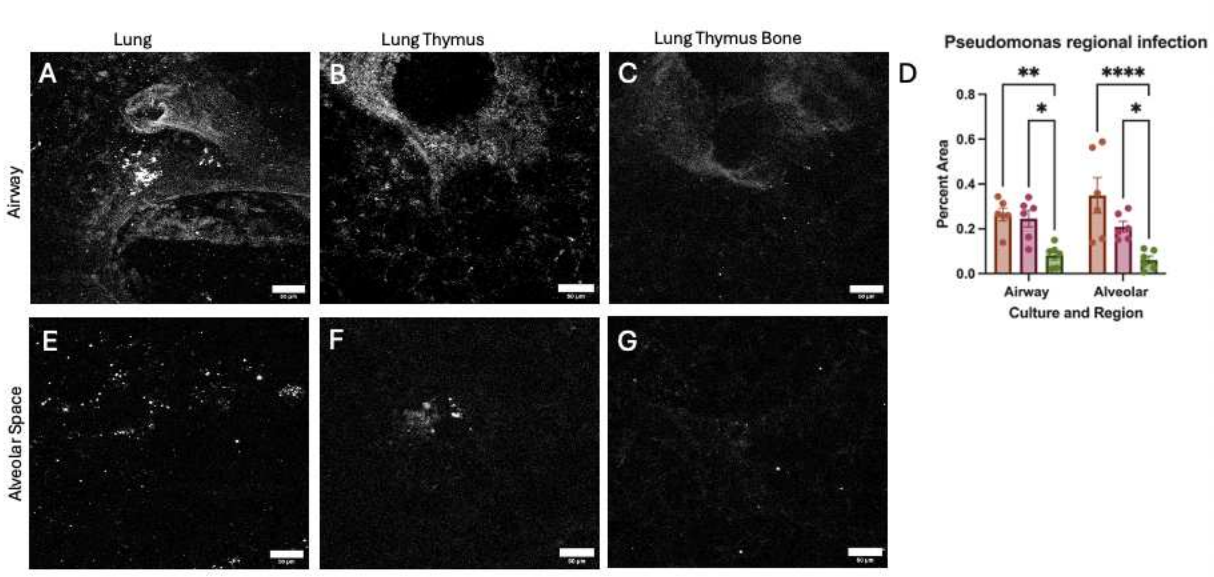

Figure 6: *P. aeruginosa* infection with culture. Vehicle lung slices had significantly increased *P. aeruginosa* infection in the airway (A) and in the alveolar space (E). Lung co-culture with thymus did not significantly alter the *P. aeruginosa* infection in either the airway (B) or the alveolar space (F). Lung co-culture with thymus and bone significantly decreased *P. aeruginosa infection* in both the airway (C) and the alveolar space (G).

Average percent area *of P. aeruginosa* in lung slices with each culture is represented in the graph (D). The orange bar represents lung cultured independently, pink represents lung with thymus, green represents lung with thymus and bone. Scale bars are 50 μm.

3.3.4 Viral Infection

Observing that bacteria, such as *P. Aeruginosa* could infect the lung, two viruses of increasing prevalence were tested in lung slices. Dengue virus did not infect the lung. Immunohistochemistry of the Dengue viral E-protein was found in macrophages on day 1 (data not shown) but did not demonstrate labelled infected lung cells. Moreover, as previously shown, immune stimulation can cause expansion of B-cells. There were no differences among B-cell populations in vehicle versus Dengue virus treated lung tissue (Supplemental Figure 5A). Plaque assays of media collected 24 and 96 h after treatment also came back with negative results, demonstrating that the virus neither survived nor replicated in lung slices (Supplemental Figure 5B). Dengue virus was attempted with the

co-culture paradigm, again demonstrating that there was no infection (Supplemental Figure 5C). Furthermore, through visualization of the Sindbis nucleocapsid protein and CD19+ B-cells, it was observed that Sindbis virus did not infect lung slices (Supplemental Figure 6).

4.3.1 Co-Culture with Resiquimod: T-cells

A TLR7/8 agonist was added to co-culture experiments for its ability to bind to a common receptor (TLR7 in mice) RNA viruses typically bind to during infection, mimicking viral infection in our slices. CD3+ T-cells were examined after 48 hours in culture. T-cell counts in lung slices treated with Resiquimod and co-cultured with thymus did not significantly increase in either the airway (Figure 7F; P = 0.1183) or alveolar space (Figure 8F; P = 0.5187) when compared to lung treated with Resiquimod. When lung slices were treated with Resiquimod and co-cultured with thymus and bone marrow, T-cells significantly increased by 151.2% (Figure 7G; P < 0.0001) in the airway and by 200.8% (Figure 8G; P = <0.0001) in the alveolar space. Furthermore, when lung slices were cultured independently and treated with Resiquimod, T-cells increased by 186.3% (Figure 7E; P = 0.0020) in the airway and by 204.8% (Figure 8E; P = 0.0047) in the alveolar space, when compared to its vehicle control. When the lung was cultured with thymus and treated with Resiquimod, T-cells increased by 106.1% (Figure 7F; P =0.0007) in the airway and 106.9% (Figure 8F; P = 0.0086) in the alveolar space, when compared to its vehicle control. Lastly, when lung slices were co-cultured with thymus and bone marrow while treated with Resiquimod, T-cells increased by 48.9% (Fig 7G; P = 0.0002) in the airway and by 72.2% (Figure 8G; P < 0.0001) in the alveolar space, when compared to its vehicle control.

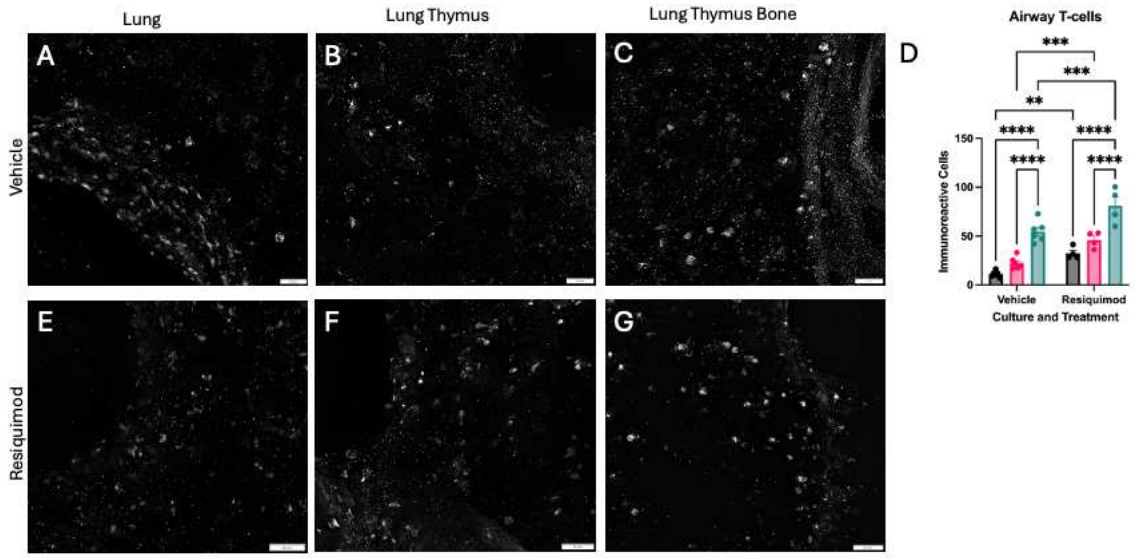

Figure 7: Airway T-cells after treatment. Lung slices cultured independently did not have a significant T-cell increase after Resiquimod treatment (E). Lung cultured with thymus did not have a significant increase in T-cells after Resiquimod treatment (F). Lung cultured with thymus had a significant increase in T-cells after Resiquimod treatment (G). Average number of T-cells with each culture is represented in the graph (D). The black bar represents lung cultured independently, pink represents lung with thymus, and teal represents lung with thymus and bone. Scale bars are 20 μm.

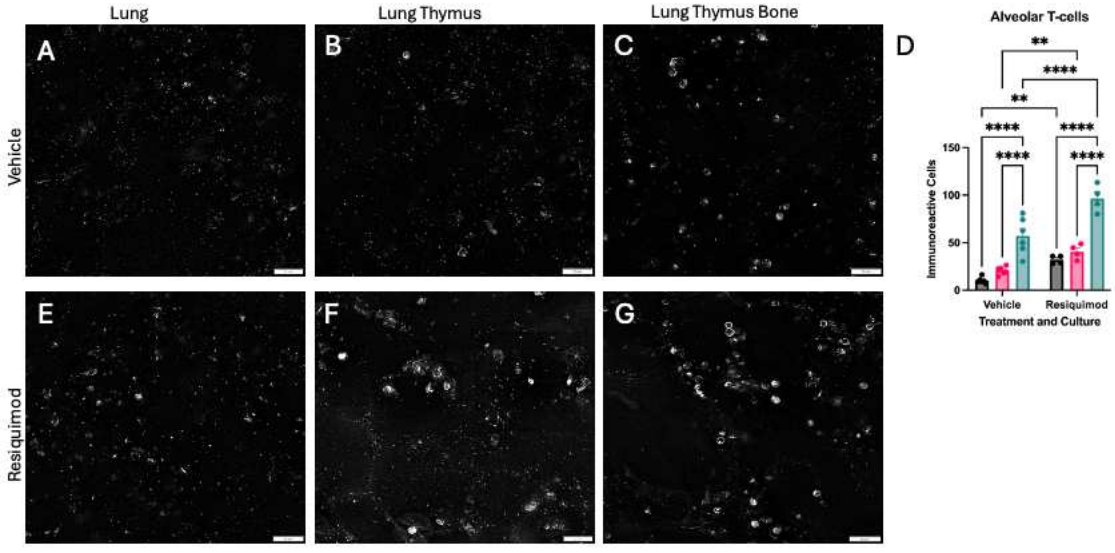

Figure 8: Alveolar T-cells after treatment. Lung slices cultured independently did not have a significant T-cell increase after Resiquimod treatment (E). Lung cultured with thymus did not have a significant increase in T-cells after Resiquimod treatment (F). Lung cultured with thymus had a significant increase in T-cells after Resiquimod treatment (G). Average number of T-cells with each culture is represented in the graph (D). The black bar represents lung cultured independently, pink represents lung with thymus, and teal represents lung with thymus and bone. Scale bars are 20 μm.

4.3.1 Co-Culture with Resiquimod: B-cells

CD19+ B-cell populations did not increase as a result of culture (P = 0.5738) but did increase as a result of treatment (P = <0.0001) (Supplemental Figure 7). Similar to the bacterial data, B-cells slightly decrease among culture paradigms, albeit insignificantly in both the vehicle and Resiquimod culture conditions. When lung slices were cultured independently and treated with Resiquimod, B-cells increased by 115.6% (P = 0.0002), compared to its vehicle control. When lung slices were cultured with thymus and treated with Resiquimod, B-cells increased by 102.8% (P = 0.0013) as compared to its vehicle control. Similarly, when lung slices were cultured with thymus and bone and treated with Resiquimod, B-cells increased by 102.9% (P = 0.0002) when compared to its vehicle control.

2.4.1 Discussion

Exposure of lung tissue to bacterial and viral agents result in activation of key immune modulators, such as B and T-cells. The current body of work tested the ability of PCLS to become infected ex vivo. When *P. Aeruginosa* was administered to the culture media, there was an apparent expansion of B-cells in the slices but limited evidence of T-cell proliferation. Immunoreactive CD3 showed there were limited resident T-cells in PCLS. Consistent with previous literature (Viana et al., 2022; Koziol-White. 2024; Cramer et al., 2022), *P. Aeruginosa* infected PCLS in the current study. Previous studies using PCLS have presented conflicting data about T-cells, typically due to protocol differences. RNA-sequencing data showed maintenance of T-cell populations in PCLS, however, samples

from that study were not perfused (Crue et al., 2023). While others reported varying T-cell levels, with most having few cells present (Stegmayr et al., 2021). As T-cell populations are diminished in PCLS, this study demonstrates a method to increase T-cell numbers in PCLS to more effectively study infection ex vivo.

To increase the T-cell population, co-culture using immune organs, such as thymus and bone, was implemented. When lungs slices are cultured independently, there are limited T-cells in the slices. A major finding in this study is that co-culturing with thymus and bone significantly increases T-cell populations in lung slices. One concern with increasing the T-cell populations using co-culture is subsequent tissue damage as T-cells are involved in inflammatory responses. Thus, tissue health was examined after co-culture using acridine orange (data not shown). Lung slices appeared healthy with viable cell populations present across all culture and co-culture paradigms. Interestingly, while lung co-culture with thymus and bone increases T-cell populations, B-cell and cKit+ cells are unaffected. Hematopoietic stem cells, mast cells, and some macrophages are all cKit+ cells. As these cells did not increase with co-culture (Supplemental Figure 2), it is not likely that co-culture by itself induces an inflammatory response. Additionally, B-cells are typically found in germinal centers associated with bronchiolar associated lymphoid tissues (BALT). Data showed that B-cells maintained the same quantity of cells and in a similar location. During a response to a pathogen or injury, B-cells can exit from germinal centers and disperse to the sites of injury (Akkaya et al., 2020). The lack of B-cell and cKit+ cell expansion suggests that co-culturing the lung with immune organs, such as bone marrow and thymus did not influence or induce inflammatory signaling.

When the co-cultures were stimulated by LPS or infected with *P. Aeruginosa* there were significant but equal increases in B-cell populations throughout the culture paradigms. Consistent with other studies, LPS is a known inducer of B-cell expansion in mice (Xu et al., 2008; Zimmerman et al., 2013). At the same time, in the current study T-cells increased as a response to treatment with LPS or *P. Aeruginosa*. PCLS co-culture with thymus and bone had the most significant increase in T-cells and while B-cells expanded, they did so in an equal manner as lung slices cultured independently. LPS is a strong stimulatory factor for antigen presenting cells, such as macrophages, inducing these cells to release pro-inflammatory cytokines. Consistent with other studies, LPS can induce a dose dependent expansion of T-cells (Tough et al., 1997; Ulmer et al., 2000). In the current study, when exogenous LPS or *P. Aeruginosa* was administered, a subsequent immune response followed in lung slices and co-cultures, validating the model to study infection ex vivo.

Interestingly, when lung slices were co-cultured with thymus and bone and infected with *P. Aeruginosa*, the degree of infection was significantly less compared to lung slices cultured independently. While immunocompetent individuals are less susceptible to severe infection with *P. Aeruginosa*, immunocompromised people, such as patients with cystic fibrosis are more susceptible to severe, chronic, and fatal infections. Studies have shown that Cystic fibrosis patients have fewer regulatory T-cells, decreasing their protection from respiratory pathogens. (Hector et al., 2015; Quigley et al., 2015). Along those lines, early protection from *P. Aeruginosa* is influenced by the presence of Th17 T-cells and their production of cytokines, such as interleukin-17A (Wu et al. 2012).

Consistent with previous reports (Omar et al., 2020; Zhang et al., 2023), the presence of T-cells influences the degree of bacterial infection in the lung and one's protection against certain pathogens. The results observed with the lung with thymus and bone co-culture indicated that T-cells play a large role in mediating infection in the lung. In the instance that there is an emergence of a new pathogen, the results of this study show that PCLS co-culture would be a more appropriate model to study and understand the microbe and potential treatments.

The results of the current study establish that PCLS can be infected with *P. Aeruginosa*. This led to experiments with 2 different viruses in culture. The two viruses used in our experiments – Dengue and Sindbis – did not infect the lung slices. Consistent with other studies, immunocompetent mice cannot easily be infected with Dengue and other arboviruses due to strong interferon responses (Sarathy et al., 2014; Marin-Lopez et al., 2019). Both Dengue and Sindbis virus are positive-sense RNA viruses that can activate TLR7 in mice. As such, studying infection in a co-culture lung slice model with a TLR7 agonist was advantageous. Resiquimod has been shown in cancer studies to increase immune cells, such as CD8+ T-cells, to tumors (Vinod et al., 2020; Zhang et al., 2023; Anfray et al., 2021). Resiquimod is known to induce a pro-inflammatory pathway like what would be activated when an RNA virus binds the same TLR7 receptors. Using this viral mimic, when lung co-cultures were treated with Resiquimod, an immune response was observed with both B-cell and T-cell populations increasing. T-cells significantly increased in the lung with thymus and bone co-culture. Current literature has shown the importance of having T-cells respond to viral infection (Risendahl-Huber et al., 2014). Compared with

the bacterial experiment results, the increased T-cell numbers in the lung cultured with bone and thymus signifies the importance of T-cells in responding to infection. The results of the Resiquimod experiments demonstrate that in the instance a RNA virus binds TLR7, the PCLS model can mobilize a significant immune response. As such, the PCLS co-culture model is an appropriate model to study infection in the instance a new viral respiratory pathogen emerges.

Increased T-cell numbers in lung slice co-cultures in the current study begs the question as to whether it was proliferation or recruitment of T-cells. When co-cultures are plated, there is a collagen overlay that separates the thymus and lung tissue. CD3+ T-cells were visualized in the collagen overlay bridge between the two organs (Supplemental Figure 1B) suggesting that cells moved out of thymus and toward lung slices. Additionally, preliminary data with media conditioned with thymus, bone, or thymus and bone did not increase the T-cell populations in lung slices. This indicates that the increases observed in T-cell populations were not a result of proliferation and are more likely due to recruitment. Although cytokine profiles were not analyzed in this study, there are studies looking at specific cytokines' roles with immune cell expansion. For instance, IFN-α has been implicated in inhibiting the proliferation of hematopoietic stem cells – cells vital for the process and commitment to the T-cell lineage (Demerdash et al., 2021). As Resiquimod only had significant increases in T-cells in the lung with thymus and bone co-culture and not the lung with thymus, IFN-α is most likely not the cytokine influencing the current data since TLR7 activation is known to induce IFN-α. The results with LPS and *P. Aeruginosa* also suggest that IFN-β is not the likely cause of the increased T-cells for the same reason.

Future experiments would be needed to elucidate what component produced in the bone is vital for increasing T-cell populations ex vivo in our PCLS co-culture paradigm.

Although infection in PCLS has been explored in the past, baseline immune cell populations have been minimally studied. However, some studies have examined the resident B-cell population in lung slices (Patlin et al., 2023). Understanding the immune cell complement in lung slices is vital to creating a comprehensive picture of PCLS uses in future research. This study demonstrates the potential of PCLS co-cultures as a model to study bacterial and viral infections. Immune cells, such as T-cells, have been implicated in various defensive mechanisms against pathogens and disease, such as their role in mucosal immunity (Shepard and McLaren, 2020; Yunis et al., 2023; Al-Talib et al., 2024). PCLS studies offer many advantages over in vivo and in vitro work with infections such as on mouse can yield an average of 60 lung slices – increasing experimental replicates and power while decreasing animal usage. This is advantageous as one mouse can be used to better understand multiple mechanisms behind specific infections and their subsequent immune responses. The technical advancement of PCLS to include co-cultures demonstrated a protective role T-cells hold in preventing infection in the lung. At the same time, maintaining a more physiologically relevant immune cell population holds for greater possibilities in the future of bacterial and viral infection studies.

CHAPTER 3: GENERAL DISCUSSION

Pseudomonas aeruginosa is the number-one hospital acquired infection, especially in intensive care units. Immunodeficient patients, such as those with Cystic Fibrosis tend to get more severe, chronic, and antibiotic-resistant infections (Liyanarachi et al., 2022; Moradali et al., 2017). Despite *P. Aeruginosa* being extensively researched, there is much to uncover about bacterial interactions and the host immune response, such as virulence factors and cell-signaling pathways. The development of antibiotics is slow and typically takes longer to develop and screen than the bacteria take to mutate. Additionally, the widespread use of antibiotics has led to the development of multi-drug-resistant strains of *P. Aeruginosa* and other bacterial pathogens. With how quickly pathogens can mutate and new pathogens can emerge, a high-throughput and effective model needs to be developed to study infections and potential treatments. Precision cut lung slices (PCLS), while maintaining cell-cell interactions and native physiology, are useful tools to studying infection. PCLS can have multiple replicates, increasing the statistical power, while using fewer animals. One animal can be used to study a multitude of treatments to test what might work. Whereas in vivo work requires multiple animals to answer the same question PCLS could answer with one animal.

From our experiments, we showed that PCLS can be infected with *P. Aeruginosa*. When looking at the immune response this infection had on the lung slices, the resident B-cell population was significantly expanded, however there was a limited T-cell population

along with a small T-cell response. In the lung, there are tissue resident memory T-cells (TRM), typically residing in the interstitial space, alveolar walls, and the lamina propria of the bronchiole (Campbell et al., 2001). TRM have been found to decline over time, making circulation of lymphocytes vital to being able to study immune responses (Carbone et al., 2023). Modeling T-cell responses ex vivo has been challenging. Numerous ex vivo lung studies are evaluating ways to generate and maintain T-cell populations in the lung, as the harsher environment of the lung along with culture may not allow for extended lifespan of T-cells within the lung. One study showed that the environment provided in the airway causes epigenetic and transcriptional changes in these T-cell populations, resulting from amino acid depletion and increased apoptosis (Uddbäck et al., 2021). Some studies showed maintenance of T-cell populations in PCLS through single cell RNA-sequencing, however, slices were obtained from human lung biopsies and slices were not perfused with a buffer through a large airway to remove red blood cells or immune cells before culture (Crue et al., 2023). Other studies found varying levels of T-cells in PCLS (Stegmayr et al., 2021). Moreover, most studies with PCLS focus on cell types other than T-cells (Koziol-White et al., 2024; Strunz et al., 2020). Through our experiments, we found a very limited T-cell population in murine PCLS, spurring experiments to try and increase these populations ex vivo.

Our T-cell findings led to experiments examining how to increase the T-cell population in lung slices. When lung is cultured with thymus and bone (LTB), T-cells increase significantly, however when cultured with thymus (LT) or bone (LB) separately, there was not a significant increase in T-cells. This is suggestive that the bone is secreting a

factor that stimulates the thymus to produce or mobilize T-cells. When PCLS are cultured, a collagen overlay is used to create an air-liquid interface and adhere the tissue to the culture dish. There is evidence that T-cells are shuttling to the lung from the thymus as they can be visualized in the collagen between the two organs. Additionally, preliminary results using pre-conditioned media (media collected from culturing thymus independently, bone independently, and bone and thymus together) did not increase T-cell populations, suggesting that the increase in T-cells was from recruitment and not proliferation. T-cells can be found in large quantities in the lymph nodes, spleen, and Peyer's patches. Lung co-culture with spleen or Peyer's patches did not increase the lung T-cell population, further indicating the importance of the bone in co-culture.

T-cells begin by committing to the lineage in the bone marrow where they then migrate to the thymus for final maturation. In the absence of a thymus, a OP9-DL1 monolayer co-culture system showed commitment of hematopoietic stem cells into both γδ-TCR+ and αβ-TCR+ T cells when cultured with bone marrow stromal cells transduced to express the Notch ligand Delta-like-1 (Schmitt et al., 2002). Artificial thymus models using bone marrow stromal cells transduced with DLL4, among other components, also committed stems cells to single-positive T-cells (Montel-Hagen et al., 2020; Lim et al., 2024). Another study found bone marrow contains a population of double-negative T-cells that upon stimulation with a TLR ligand, have robustly accelerated proliferation through the section of IL-1β by myeloid cells (Yamamoto et al., 2019). These studies show that components provided by bone marrow are vital for T-cell differentiation and maturation

and that without bone marrow, T-cells would not undergo full selection to single positive T-cells.

Although T-cells increased as a result of LTB co-culture, there was no change in B-cell populations. Cytokine profiles were not assessed in these experiments. However, as IL-6 is a known cytokine in the bone marrow involved in the differentiation of B-cells, the observed results showing that LTB co-culture had equal populations of B-cells, instead of increased, to both the L and LT cultures suggests that interluekin-6 (IL-6) did not play a role in lung co-cultures. Both the thymus and bone marrow secrete interleukin-7 (IL-7), a key cytokine in T-cell proliferation and differentiation. As T-cells did not significantly increase in the LT co-culture, it can be inferred that IL-7 did not influence T-cell populations in co-cultures. When the co-cultures were stimulated with LPS or *P. Aeruginosa*, potent IFN-β inducers, T-cell counts in the LTB co-culture were significantly increased. As both the thymus and bone marrow can respond to IFN-β, and the LT co-culture did not respond as significantly to LPS or bacterial stimulation, it can be inferred that IFN-β was not responsible for the T-cell increase seen in the LTB co-culture. One study looked at LPS-independent inflammatory responses of *P. Aeruginosa*, determining that a virulence factor, exoenzyme S, a potent mitogen, can directly stimulate T-cells (Epelman et al., 2002). This is suggestive, as LPS and *P. Aeruginosa* increased T-cell populations to the same extent, that exoenzyme S was not involved with increasing T-cells in any infected culture. Further investigation would need to examine what cytokines, chemokines, or growth factors were secreted from the bone that influenced the LTB co-culture to have T-cell increases but not B-cells.

T-cells are vital for immune responses during bacterial and viral infection as they help with the neutralization and phagocytosis of harmful pathogens through signaling to other immune cells. When T-cells were confirmed in the PCLS LTB co-culture, lung was treated with LPS or infected with *P. Aeruginosa*. In the LTB co-culture, *P. Aeruginosa* infection was significantly ameliorated compared to lung cultured independently. Similarly, studies have shown that T-cells play a vital role in protection against *P. Aeruginosa* infection. Myeloid-derived suppressor cells (MDSCs), typically induced by the flagellin of *P. Aeruginosa,* are known to suppress T-cell responses. One study speculated that *P. Aeruginosa* uses that pathway to avoid the host immune response (Rieber et al., 2013). It has also been shown that interleukin-17 (IL-17), a cytokine involved in the Th17 response, plays a role in early protection of the host from infection (Liu et al., 2013). It is also known that cystic fibrosis patients are more susceptible to chronic *P. Aeruginosa* infection due to decreased regulatory T-cells (Hector et al., 2015). These studies suggest that T-cells play an important role in protecting the host from *P. Aeruginosa* infection, which was observed in our LTB co-culture model infected with bacteria.

P. Aeruginosa is known to cause more severe infections in males, with the males having a higher mortality rate than females. Additionally, males are more likely to develop respiratory bacterial infections in general. However, cystic fibrosis patients are more likely to have severe *P. Aeruginosa* infections compared to immunocompetent individuals. Although the prevalence of cystic fibrosis is about equal in males and females, females are more likely to develop severe and chronic infections (Wang et al., 2024; Vahedi et al., 2016, Harness-Brumley et al., 2014). It is important to note that while *P. Aeruginosa* infection

was evident in the lung slices, there were no observed sex differences. Both males and females had similar levels of infection and responses to LTB co-culture (Supplemental Figure 8). This could potentially be due to the media the tissue was cultured in. Although the CTS media does not contain any steroid hormones, the B27 supplement used contains corticosterone and progesterone, which may have some anti-inflammatory effects that may have influenced cellular responses. The media used in the current studies did not contain phenol red, which contains an estrogenic contaminant that is known to alter physiological features observed in some in vitro studies. Animal sera common to some culture media were not used in any media for these studies due to their potential to contain a variety of antibodies, proteins, and growth factors that could introduce variability. As sex differences were not detected; it is interesting to speculate whether estradiol or testosterone added to culture media would have physiological effects.

As we were able to infect a lung slice with bacteria, the question became, could we infect the lung with virus. SARS-Co-V2, Sindbis, and Dengue virus are all positive-sense RNA viruses. In 2020, SARS-Co-V2 caused a major health crisis globally. Although not at pandemic levels currently, Dengue infections have strikingly increased since 2000 as climate change makes northern regions warmer. Preliminary results (Patlin et al., unpublished) demonstrated that SARS-Co-V2 could infect lung slices. However, the increasing prevalence of Dengue infections spurred the idea to see if Dengue virus could infect PCLS.

In our experiments, the Dengue virus did not show any signs of infection in the lung slices. Immunohistochemistry of the viral E-protein and of CD19+ B-cells indicated that

the virus was not replicating and surviving. As B-cells did not increase as a response to culturing with virus, this showed that there was no endogenous response to infection. Furthermore, results from the plaque assay indicate that the virus was not replicating and surviving in lung slices as there was no detectable virus after 24 hours in culture. The lack of infection with Dengue virus shows that lung slices might not be an appropriate model to study this pathogen. This was also the same story for lung slices infected with Sindbis virus as CD19+ B cells did not increase nor was there any indication of infection through labeling of the viral nucleocapsid protein.

Other studies have shown that immunocompetent mice are not susceptible to infection with Dengue virus due to active interferon responses (Sarathy et al., 2014; Marin-Lopez et al., 2019). AG129 mice have been shown to be susceptible to all serotypes (1-4) of dengue virus as they lack receptors for IFN α/β/γ (Baldon et al., 2022; Kayesh and Kohara, 2022). Studies using aged AG129 mice showed that they are more susceptible to dengue infection, have more severe infections, and higher mortality rates (Siddqui et al., 2024). Others found that immunocompetent mice are susceptible to Dengue infection only in specific circumstances (Jacome et al., 2019; Goncalves et al., 2012). One study showed that C57BL/6 and BALB/c mice at suckling age inoculated with Dengue virus were more susceptible to infection and had marked differences in immune responses, with C57 mice having upregulated Th1 responses in comparison to BALB/c mice (Byrne et al., 2021). Additionally, Dengue virus has infected in vivo humanized mouse models when they were transplanted with human lung or with human immune components, such as bone marrow and thymus (Wahl et al., 2019). Dengue infection in mice could be influenced by the

serotype (1-4) and the diversity of the viral strains within each serotype. Dengue pathogenesis is still relatively unknown as to what receptors are needed for infection. The lack of infection seen in our study could be the result of a few factors, such as that the virus was human adapted, Dengue is not a known respiratory pathogen, the lung slices might be lacking the receptors needed for infection, and that the lung slices have an active interferon response.

Sindbis virus is a zoonotic virus maintained in wild-bird populations and endemically circulates through mosquitoes. The number of active infections in humans typically correlates with bird migration and peak mosquito populations (Ziegler et al., 2019). In vivo murine studies have shown that Sindbis can cause an active infection, however not in lung. Sindbis virus is typically associated with infecting nervous tissue, such as the brain and spinal cord, causing encephalitis, encephalomyelitis, and paralysis (Klimstra et al., 1999; Jackson et al., 1988; Thach et al., 2000). In a clinical case report, 36% of patients infected with Sindbis experienced upper respiratory symptoms, such as sore throat and a cough (Jussi et al., 2011). With the experiments in lung slices, Sindbis virus did not cause an infection. We saw this through no increase of resident B-cells as well as no labeling of the nucleocapsid protein. Although causing some respiratory symptoms in one study, Sindbis virus is not a known respiratory pathogen. The molecular mechanism of Sindbis is not well defined, but recent studies have begun to elucidate a specific pathway that is required for Sindbis virus to cause infection. One study shows that Sindbis capsid protein has to interact with interleukin receptor associated kinase-1 (IRAK1) to systemically disseminate (Landers et al., 2024). IRAK1 activation leads to the increased

transcription of nuclear factor (NF)-kB dependent genes, which has been shown to suppress the production of interferons and downregulate interferon receptors, decreasing the hosts antiviral response (Kim et al., 2024). Although the Sindbis virus did not infect lung slices, we did not run a positive control, such as a culture of brain or spinal cord, so we cannot determine if it was the strain of Sindbis or the tissue type we were trying to infect. However, there are a few reasons that Sindbis virus might not have infected the lung such that it is not a respiratory pathogen, or the lung slices did not contain the right receptors for infection. Future experiments would have to elucidate if IRAK-1 is present in lung slices.

Although we did not get viral infection in our lung slices, T-cells have been shown to help prevent Dengue infection (Weiskopf and Sette, 2014; Zompi et al., 2014). With previous evidence, we know that PCLS do not contain a large population of T-cells, thus the lack of infection of Dengue was not a result of a T-cell response. However, that begged the question as to what the T-cell response looked like with viral infection in the presence of co-cultures.

Sars-Co-V2, Dengue, and Sindbis virus are all positive sense RNA viruses. As such, RNA viruses can activate Toll-like receptor 7 (TLR7), one of many essential receptors for immune responses. For the current study, Resiquimod (R-848) was used to mimic an RNA virus infection as it can activate TLR7. Resiquimod is a synthetic compound that can modify the immune response as it is a potent inducer of interferon alpha (IFN-α) and has been shown to increase immune responses by binding to TLR7/8 (Salinas et al., 2020; Dockrell and Kinghorn, 2001). Few studies have used Resiquimod in respiratory research. However, one study found that in the lungs of adult and neonate mice treated with

Resiquimod there were increased levels of IL-6 in the bronchoalveolar lavage fluid (Makris and Johansson, 2021). This is suggestive that Resiquimod triggers a similar pro-inflammatory pathway that would be seen with viral infections. Resiquimod has primarily been implemented in cancer studies, specifically with the recruitment of CD8+ T-cells to tumors, in addition to other immune responses (Vinod et al., 2020; Zhang et al., 2023; Anfray et al., 2021). As Resiquimod has the ability to mimic a potential infection pathway that the Dengue, Sindbis, or Sars-Co-V2 viruses would have activated, it was an appropriate model to test ex vivo lung slice's ability to respond to pathogens.

The current study did not focus on any cytokine profiles within each of the co-cultures. However, when the co-cultures were stimulated with Resiquimod, a potent IFN-α inducer, T-cell counts in the LTB co-culture were significantly increased. As both the thymus and bone marrow can respond to IFN-α, and the LT co-culture did not respond as significantly to Resiquimod, it can be inferred that IFN-α was not responsible for the T-cell increase seen in the LTB co-culture. Additionally, in-vitro studies have shown that viral mimics that induce the production of IFN-α, such as polyI:C, inhibit proliferation of hematopoietic stems cells (Demerdash et al., 2021). As we saw significantly increased T-cell populations in the LTB co-culture treated with Resiquimod, IFN-α was not a probable cause for the results observed. Additionally, if IFN-α was what induced the increased T-cell populations in the LTB co-culture, then the LT co-culture should have had equal levels of T-cells. Future experiments would need to elucidate what cytokine, chemokine, and growth factors are secreted by the LTB co-culture that influences the observed T-cell increases in lung slices.

Through our experiments, we showed that lung slices can be infected with bacteria, such as *P. Aeruginosa*. Lung slices do not have a population of T-cells that would replicate in-vivo populations and thus infection studies in PCLS without co-culture have limitations. When lung is co-cultured with thymus and bone, there are no changes in resident B-cell or cKit+ cell populations but there is an increase in T-cells. The increase in T-cells with the lung cultured with thymus and bone ameliorated the *P. Aeruginosa* infection observed. When Dengue and Sindbis viruses were used, it was determined that they did not infect lung slices. However, a viral mimic could induce the immune pathway through TLR7. Lung cultured with thymus and bone had significant increases in T-cells. These results demonstrate that in the instance that another pathogen emerges, we have a model that can appropriately mimic immune cell populations and interactions that would be seen in vivo.

CHAPTER 4: SUPPLEMENTAL FIGURES

Figure 1: Co-culture plating and collagen overlay bridge

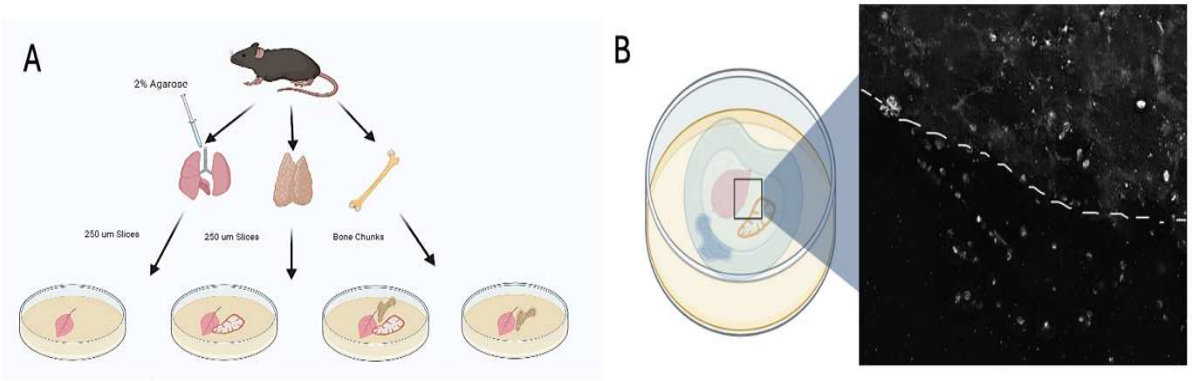

Supplemental figure 1: Co-cultures and collagen overlay. A diagram of organ collection and subsequent plating is shown (A). Tissue does not need to be touching but was relatively close together (left B). Collagen overlay between lung and thymus suggests recruitment of CD3+ T-cells from thymus to lung (right B) White dashed line represents the border of the lung (top) and the collagen overlay (bottom)

Figure 2: Co-culture does not influence cKit+ cell populations in lung slices

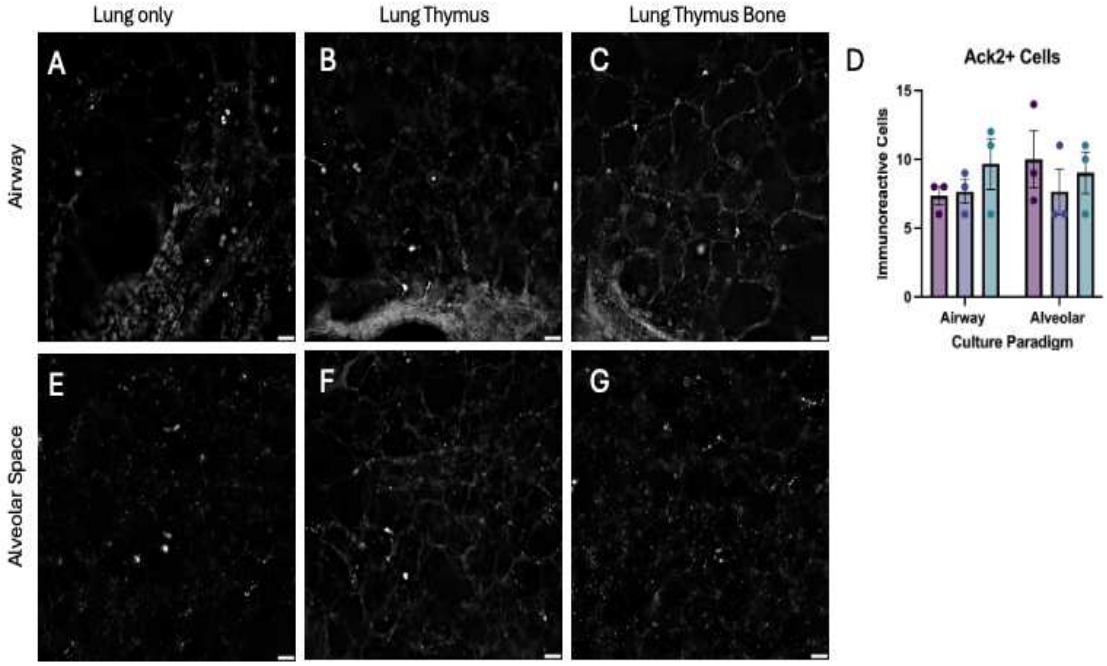

Supplemental figure 2: cKit+ (ACK2) cells in co-culture. Lung slices cultured independently does not have any significant differences in cKit+ cell population across co-cultures in the airways (A-C) or the alveolar space (E-G). Average number of cKit+ cells (hematopoietic stem cells, mast cells, macrophages) with each culture is represented (D). The dark purple represents lung cultured independently, the dark blue represents lung with thymus, and the teal bar represents lung with thymus and bone. N=3 for all groups. Scale bars are 20 μm.

Figure 3: Co-culture does not influence B-cell population in lung slices among cultures

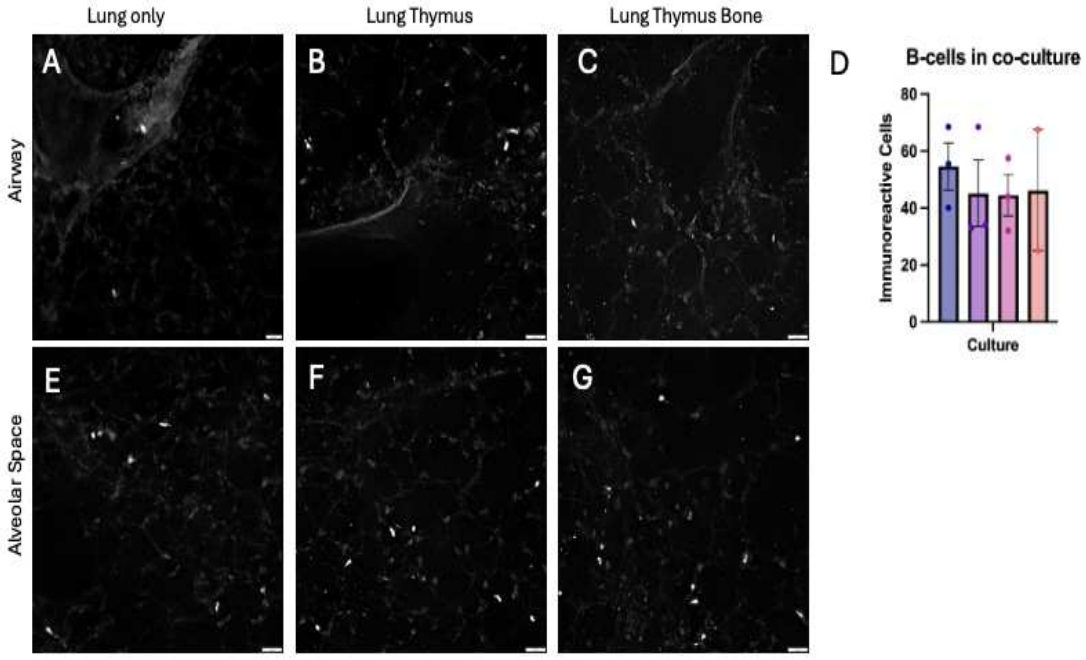

Supplemental figure 3: CD19+ B-cells in co-culture. Lung slices cultured independently did not have any significant differences in B-cell populations across co-cultures in the airways (A-C) or the alveolar space (E-G). Average number of B-cells+ cells in the entire lung slice is with each culture is represented (D). The dark blue represents lung cultured independently, the dark purple represents lung with thymus, the pink bar represents lung with thymus and bone and the orange bar represents lung with bone. N=3 for all groups except lung with bone. Scale bars are 20 μm.

Figure 4: *P. Aeruginosa* and LPS induce expansion of B-cell populations to an equal extent among cultures

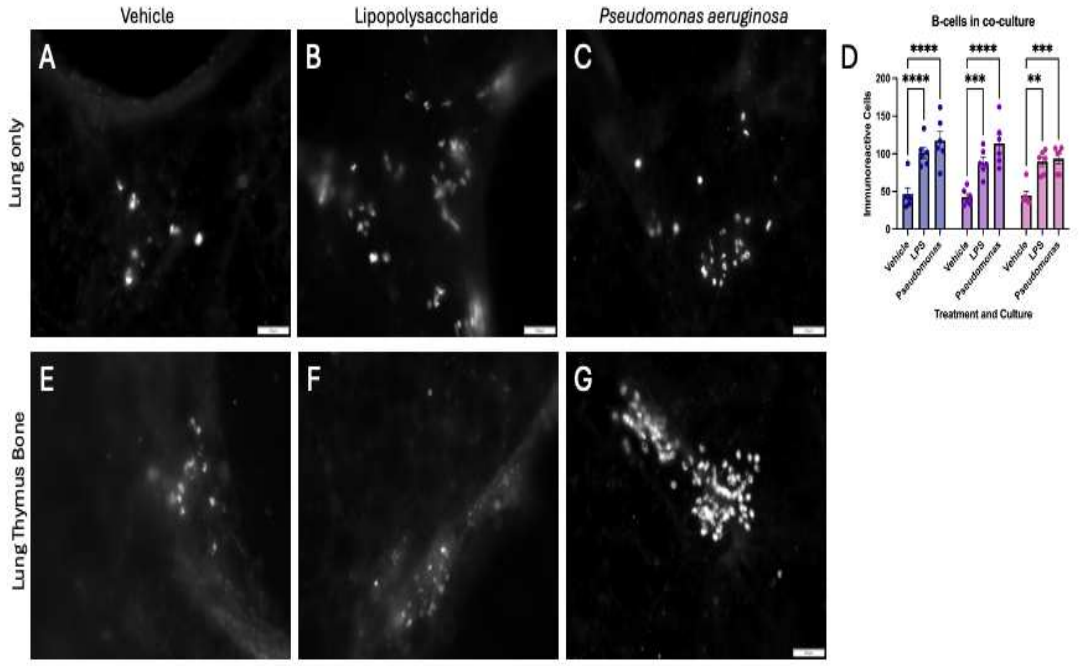

Supplemental figure 4: B-cells after treatment. Vehicle lung slices (A) had significant B-cell increases with LPS (B) and *P. aeruginosa* (C). Similarly, lung with thymus and bone (E) had significant increases in B-cells with LPS (F) and *P. aeruginosa* (G). There were no significant differences in B-cell increases between LPS and *P. aeruginosa* and no significant differences between cultures. Average number of B-cells with each culture are represented in the graph (D). The blue bar represents lung cultured independently across treatments, dark purple represents lung with thymus across treatments, and teal represents lung with thymus and bone across treatments. Scale bars are 20 μm.

Figure 5: Dengue virus did not infect lung slices

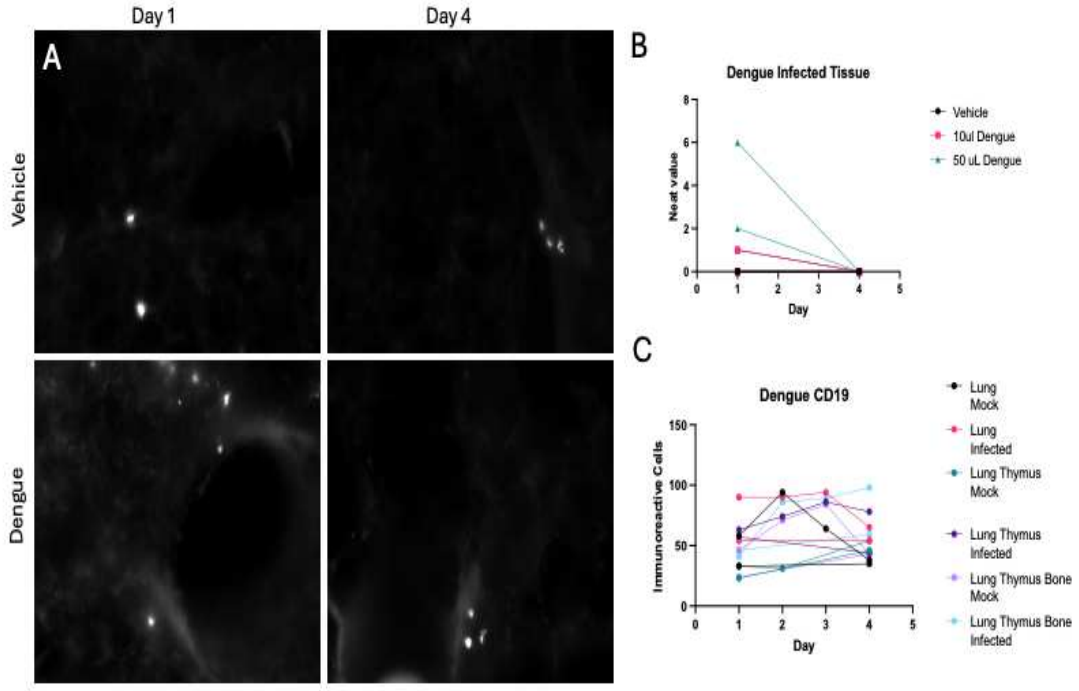

Supplemental figure 5: Dengue virus in lung slices. CD19 B-cells did not expand with treatment of lung slices with Dengue virus indicating no infection is present (A). Plaque assay data indicates Dengue virus is not surviving or replicating (B). When Dengue was placed in the co-culture paradigm, there was no expansion of B-cells in treated tissue indicating the virus is not replicating and surviving in lung (C).

Figure 6: Sindbis virus did not infect lung slices

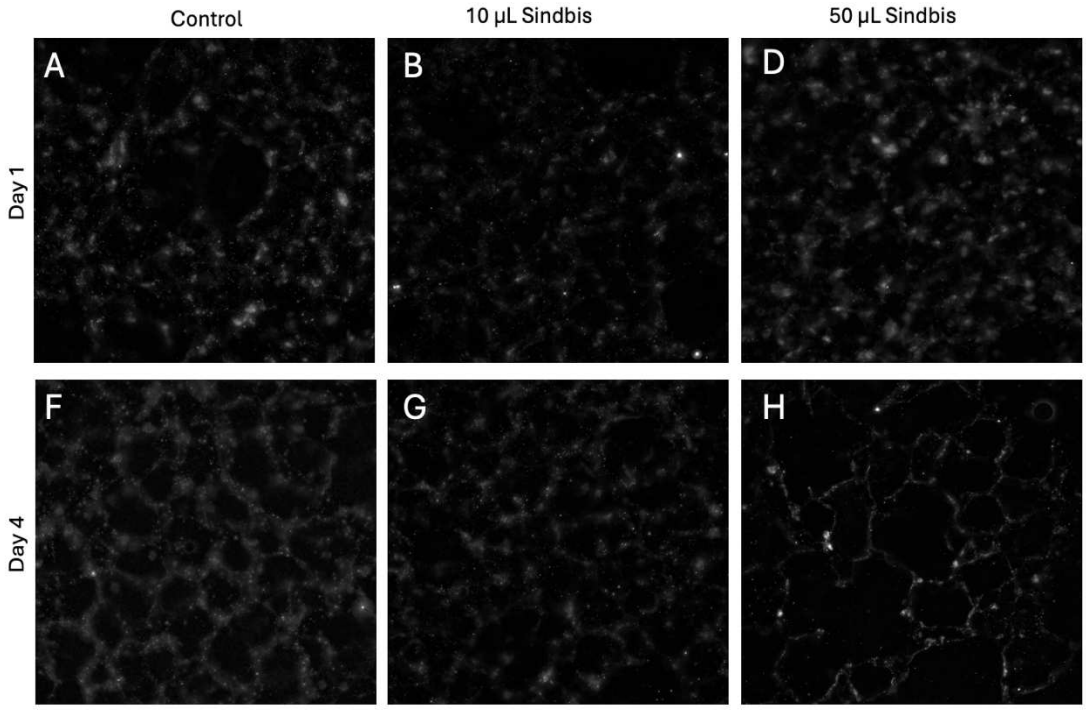

Supplemental figure 6: Sindbis virus in lung slices. Immunohistochemistry for the Sindbis nucleocapsid protein did not reveal any signs of infection in lung slices on day 1 (A-D) or after 4 days (F-H)

Figure 7: Resiquimod induced expansion of B-cell populations to an equal extent among cultures

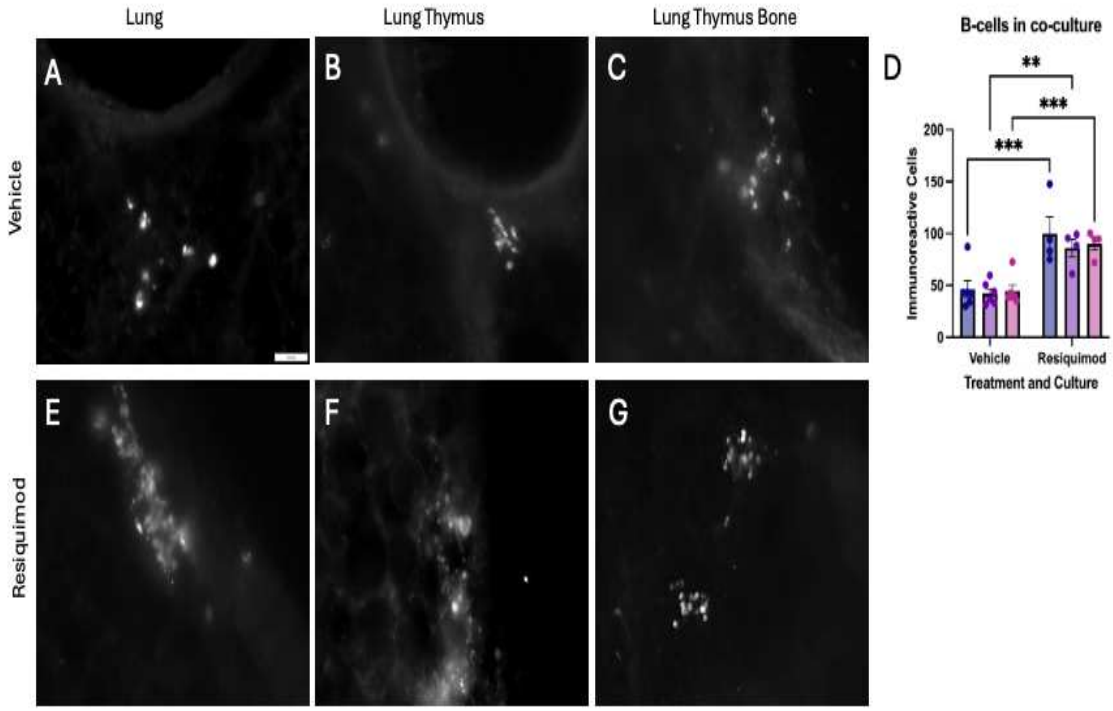

Supplemental figure 7: B-cells after treatment. Lung slices cultured independently had significant increases in B-cells after Resiquimod treatment (E). Lung slices cultured with thymus had significant increases in B-cells after Resiquimod treatment (F). Lung slices cultured with thymus and bone had significant increases in B-cells after Resiquimod treatment (G). There were no differences in B-cells across cultures (A-C) or after treatment across cultures (E-G). Scale bars are 20 μm.

Figure 8: No sex differences were observed with Pseudomonas infection

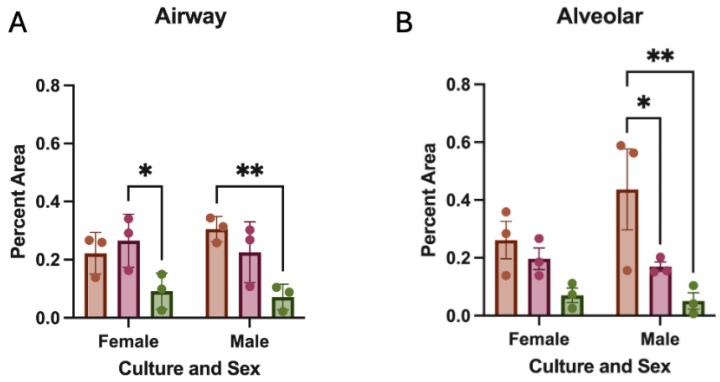

Supplemental figure 8: No sex differences were observed with Pseudomonas Infection: There were no significant differences in P. Aeruginosa infection in either the airway (A) or the alveolar space(B). There were also no sex differences among culture paradigms in P. Aeruginosa infected tissue

REFERENCES

Akkaya, M., Kwak, K., & Pierce, S. K. (2020). B cell memory: building two walls of protection against pathogens. *Nat Rev Immunol, 20*(4), 229-238. doi:10.1038/s41577-019-0244-2

Al-Talib, M., Dimonte, S., & Humphreys, I. R. (2024). Mucosal T-cell responses to chronic viral infections: Implications for vaccine design. *Cell Mol Immunol*. doi:10.1038/s41423-024-01140-2

Alfaro-Moreno, E., Nawrot, T. S., Vanaudenaerde, B. M., Hoylaerts, M. F., Vanoirbeek, J. A., Nemery, B., & Hoet, P. H. (2008). Co-cultures of multiple cell types mimic pulmonary cell communication in response to urban PM10. *Eur Respir J, 32*(5), 1184-1194. doi:10.1183/09031936.00044008

Anfray, C., Mainini, F., Digifico, E., Maeda, A., Sironi, M., Erreni, M., . . . Andón, F. T. (2021a). Intratumoral combination therapy with poly(I:C) and resiquimod synergistically triggers tumor-associated macrophages for effective systemic antitumoral immunity. *J Immunother Cancer, 9*(9). doi:10.1136/jitc-2021-002408

Anfray, C., Mainini, F., Digifico, E., Maeda, A., Sironi, M., Erreni, M., . . . Andón, F. T. (2021b). Intratumoral combination therapy with poly(I:C) and resiquimod

synergistically triggers tumor-associated macrophages for effective systemic antitumoral immunity. *J Immunother Cancer, 9*(9). doi:10.1136/jitc-2021-002408

Baldon, L. V. R., de Mendonça, S. F., Ferreira, F. V., Rezende, F. O., Amadou, S. C. G., Leite, T. H. J. F., . . . Ferreira, A. G. A. (2022a). AG129 Mice as a Comprehensive Model for the Experimental Assessment of Mosquito Vector Competence for Arboviruses. *Pathogens, 11*(8). doi:10.3390/pathogens11080879

Baldon, L. V. R., de Mendonça, S. F., Ferreira, F. V., Rezende, F. O., Amadou, S. C. G., Leite, T. H. J. F., . . . Ferreira, A. G. A. (2022b). AG129 Mice as a Comprehensive Model for the Experimental Assessment of Mosquito Vector Competence for Arboviruses. *Pathogens, 11*(8). doi:10.3390/pathogens11080879

Banerjee, S. K., Huckuntod, S. D., Mills, S. D., Kurten, R. C., & Pechous, R. D. (2019). Modeling Pneumonic Plague in Human Precision-Cut Lung Slices Highlights a Role for the Plasminogen Activator Protease in Facilitating Type 3 Secretion. *Infect Immun, 87*(8). doi:10.1128/IAI.00175-19

Brandstadter, J. D., & Maillard, I. (2019). Notch signalling in T cell homeostasis and differentiation. *Open Biol, 9*(11), 190187. doi:10.1098/rsob.190187

Byrne, A. B., García, A. G., Brahamian, J. M., Mauri, A., Ferretti, A., Polack, F. P., & Talarico, L. B. (2021). A murine model of dengue virus infection in suckling C57BL/6 and BALB/c mice. *Animal Model Exp Med, 4*(1), 16-26. doi:10.1002/ame2.12145

Campbell, J. J., Brightling, C. E., Symon, F. A., Qin, S., Murphy, K. E., Hodge, M., . . . Wardlaw, A. J. (2001). Expression of chemokine receptors by lung T cells from normal and asthmatic subjects. *J Immunol, 166*(4), 2842-2848. doi:10.4049/jimmunol.166.4.2842

Carbone, F. R. (2023). Unique properties of tissue-resident memory T cells in the lungs: implications for COVID-19 and other respiratory diseases. *Nat Rev Immunol, 23*(5), 329-335. doi:10.1038/s41577-022-00815-z

Craig, A., Mai, J., Cai, S., & Jeyaseelan, S. (2009). Neutrophil recruitment to the lungs during bacterial pneumonia. *Infect Immun, 77*(2), 568-575. doi:10.1128/IAI.00832-08

Cramer, N., Nawrot, M. L., Wege, L., Dorda, M., Sommer, C., Danov, O., . . . Tümmler, B. (2022). Competitive fitness of. *Front Cell Infect Microbiol, 12*, 992214. doi:10.3389/fcimb.2022.992214

Crue, T., Lee, G. Y., Peng, J. Y., Schaunaman, N., Agraval, H., Day, B. J., . . . Chu, H. W. (2023). Single cell RNA-sequencing of human precision-cut lung slices: A novel approach to study the effect of vaping and viral infection on lung health. *Innate Immun, 29*(5), 61-70. doi:10.1177/17534259231181029

Dagenais, A., Villalba-Guerrero, C., & Olivier, M. (2023). Trained immunity: A "new" weapon in the fight against infectious diseases. *Front Immunol, 14*, 1147476. doi:10.3389/fimmu.2023.1147476

Davidovich, N., Huang, J., & Margulies, S. S. (2013). Reproducible uniform equibiaxial stretch of precision-cut lung slices. *Am J Physiol Lung Cell Mol Physiol, 304*(4), L210-220. doi:10.1152/ajplung.00224.2012

Debbabi, H., Ghosh, S., Kamath, A. B., Alt, J., Demello, D. E., Dunsmore, S., & Behar, S. M. (2005). Primary type II alveolar epithelial cells present microbial antigens to antigen-specific CD4+ T cells. *Am J Physiol Lung Cell Mol Physiol, 289*(2), L274-279. doi:10.1152/ajplung.00004.2005

Delmotte, P., & Sanderson, M. J. (2006). Ciliary beat frequency is maintained at a maximal rate in the small airways of mouse lung slices. *Am J Respir Cell Mol Biol, 35*(1), 110-117. doi:10.1165/rcmb.2005-0417OC

Demerdash, Y., Kain, B., Essers, M. A. G., & King, K. Y. (2021). Yin and Yang: The dual effects of interferons on hematopoiesis. *Exp Hematol, 96*, 1-12. doi:10.1016/j.exphem.2021.02.002

Dockrell, D. H., & Kinghorn, G. R. (2001). Imiquimod and resiquimod as novel immunomodulators. *J Antimicrob Chemother, 48*(6), 751-755. doi:10.1093/jac/48.6.751

Ebsen, M., Mogilevski, G., Anhenn, O., Maiworm, V., Theegarten, D., Schwarze, J., & Morgenroth, K. (2002). Infection of murine precision cut lung slices (PCLS) with respiratory syncytial virus (RSV) and chlamydophila pneumoniae using the

Krumdieck technique. *Pathol Res Pract, 198*(11), 747-753. doi:10.1078/0344-0338-00331

Epelman, S., Neely, G. G., Ma, L. L., Gjomarkaj, M., Pace, E., Melis, M., . . . Mody, C. H. (2002). Distinct fates of monocytes and T cells directly activated by Pseudomonas aeruginosa exoenzyme S. *J Leukoc Biol, 71*(3), 458-468.

Freeman, B. A., & O'Neil, J. J. (1984). Tissue slices in the study of lung metabolism and toxicology. *Environ Health Perspect, 56*, 51-60. doi:10.1289/ehp.845651

Garis, M., & Garrett-Sinha, L. A. (2020). Notch Signaling in B Cell Immune Responses. *Front Immunol, 11*, 609324. doi:10.3389/fimmu.2020.609324

Gonçalves, D., de Queiroz Prado, R., Almeida Xavier, E., Cristina de Oliveira, N., da Matta Guedes, P. M., da Silva, J. S., . . . Aquino, V. H. (2012). Immunocompetent mice model for dengue virus infection [corrected]. *ScientificWorldJournal, 2012*, 525947. doi:10.1100/2012/525947

Gopallawa, I., Dehinwal, R., Bhatia, V., Gujar, V., & Chirmule, N. (2023). A four-part guide to lung immunology: Invasion, inflammation, immunity, and intervention. *Front Immunol, 14*, 1119564. doi:10.3389/fimmu.2023.1119564

Harness-Brumley, C. L., Elliott, A. C., Rosenbluth, D. B., Raghavan, D., & Jain, R. (2014). Gender differences in outcomes of patients with cystic fibrosis. *J Womens Health (Larchmt), 23*(12), 1012-1020. doi:10.1089/jwh.2014.4985

Hector, A., Schäfer, H., Pöschel, S., Fischer, A., Fritzsching, B., Ralhan, A., . . . Hartl, D. (2015). Regulatory T-cell impairment in cystic fibrosis patients with chronic pseudomonas infection. *Am J Respir Crit Care Med, 191*(8), 914-923. doi:10.1164/rccm.201407-1381OC

Jackson, A. C., Moench, T. R., Trapp, B. D., & Griffin, D. E. (1988). Basis of neurovirulence in Sindbis virus encephalomyelitis of mice. *Lab Invest, 58*(5), 503-509.

Janeway, C., Travers, P., Walport, M., & Shlomchik, M. (2001). Generation of lymphocytes in bone marrow and thymus. In G. Science (Ed.), *Immunobiology: The Immune System in Health and Disease.* (5th ed.). New York: Garland Science.

Johnston, S. L., Goldblatt, D. L., Evans, S. E., Tuvim, M. J., & Dickey, B. F. (2021). Airway Epithelial Innate Immunity. *Front Physiol, 12*, 749077. doi:10.3389/fphys.2021.749077

Jose, J., Przybyla, L., Edwards, T. J., Perera, R., Burgner, J. W., & Kuhn, R. J. (2012). Interactions of the cytoplasmic domain of Sindbis virus E2 with nucleocapsid cores promote alphavirus budding. *J Virol, 86*(5), 2585-2599. doi:10.1128/JVI.05860-11

Jácome, F. C., Caldas, G. C., Rasinhas, A. D. C., de Almeida, A. L. T., de Souza, D. D. C., Paulino, A. C., . . . Barreto-Vieira, D. F. (2021). Immunocompetent Mice Infected by Two Lineages of Dengue Virus Type 2: Observations on the Pathology of the Lung, Heart and Skeletal Muscle. *Microorganisms, 9*(12). doi:10.3390/microorganisms9122536

Kayesh, M. E. H., & Tsukiyama-Kohara, K. (2022). Mammalian animal models for dengue virus infection: a recent overview. *Arch Virol, 167*(1), 31-44. doi:10.1007/s00705-021-05298-2

Kim, K. M., Hwang, N. H., Hyun, J. S., & Shin, D. (2024). Recent Advances in IRAK1: Pharmacological and Therapeutic Aspects. *Molecules, 29*(10). doi:10.3390/molecules29102226

Klimstra, W. B., Ryman, K. D., Bernard, K. A., Nguyen, K. B., Biron, C. A., & Johnston, R. E. (1999). Infection of neonatal mice with sindbis virus results in a systemic inflammatory response syndrome. *J Virol, 73*(12), 10387-10398. doi:10.1128/JVI.73.12.10387-10398.1999

Koziol-White, C. (2022). Human Precision-Cut Lung Slices: Generation of and Measurement of Contractility and Relaxation of Small Airways. *Methods Mol Biol, 2506*, 111-117. doi:10.1007/978-1-0716-2364-0_8

Koziol-White, C., Gebski, E., Cao, G., & Panettieri, R. A. (2024). Precision cut lung slices: an integrated ex vivo model for studying lung physiology, pharmacology, disease pathogenesis and drug discovery. *Respir Res, 25*(1), 231. doi:10.1186/s12931-024-02855-6

Lam, M., Lamanna, E., Organ, L., Donovan, C., & Bourke, J. E. (2023). Perspectives on precision cut lung slices-powerful tools for investigation of mechanisms and

therapeutic targets in lung diseases. *Front Pharmacol, 14*, 1162889. doi:10.3389/fphar.2023.1162889

Landers, V. D., Thomas, M., Isom, C. M., Karki, D., & Sokoloski, K. J. (2024). Capsid protein mediated evasion of IRAK1-dependent signalling is essential to Sindbis virus neuroinvasion and virulence in mice. *Emerg Microbes Infect, 13*(1), 2300452. doi:10.1080/22221751.2023.2300452

Li, G., Cohen, J. A., Martines, C., Ram-Mohan, S., Brain, J. D., Krishnan, R., . . . Bai, Y. (2020). Preserving Airway Smooth Muscle Contraction in Precision-Cut Lung Slices. *Sci Rep, 10*(1), 6480. doi:10.1038/s41598-020-63225-y

Lim, S., J F van Son, G., Wisma Eka Yanti, N. L., Andersson-Rolf, A., Willemsen, S., Korving, J., . . . Clevers, H. (2024). Derivation of functional thymic epithelial organoid lines from adult murine thymus. *Cell Rep, 43*(4), 114019. doi:10.1016/j.celrep.2024.114019

Liu, G., Betts, C., Cunoosamy, D. M., Åberg, P. M., Hornberg, J. J., Sivars, K. B., & Cohen, T. S. (2019). Use of precision cut lung slices as a translational model for the study of lung biology. *Respir Res, 20*(1), 162. doi:10.1186/s12931-019-1131-x

Liyanarachi, K. V., Solligård, E., Mohus, R. M., Åsvold, B. O., Rogne, T., & Damås, J. K. (2022). Incidence, recurring admissions and mortality of severe bacterial infections and sepsis over a 22-year period in the population-based HUNT study. *PLoS One, 17*(7), e0271263. doi:10.1371/journal.pone.0271263

Lo, B., Hansen, S., Evans, K., Heath, J. K., & Wright, J. R. (2008). Alveolar epithelial type II cells induce T cell tolerance to specific antigen. *J Immunol, 180*(2), 881-888. doi:10.4049/jimmunol.180.2.881

Lyons-Cohen, M. R., Thomas, S. Y., Cook, D. N., & Nakano, H. (2017). Precision-cut Mouse Lung Slices to Visualize Live Pulmonary Dendritic Cells. *J Vis Exp*(122). doi:10.3791/55465

Makris, S., & Johansson, C. (2021). R848 or influenza virus can induce potent innate immune responses in the lungs of neonatal mice. *Mucosal Immunol, 14*(1), 267-276. doi:10.1038/s41385-020-0314-6

Marques, R. E., Guabiraba, R., Del Sarto, J. L., Rocha, R. F., Queiroz, A. L., Cisalpino, D., . . . Teixeira, M. M. (2015). Dengue virus requires the CC-chemokine receptor CCR5 for replication and infection development. *Immunology, 145*(4), 583-596. doi:10.1111/imm.12476

Marín-Lopez, A., Calvo-Pinilla, E., Moreno, S., Utrilla-Trigo, S., Nogales, A., Brun, A., . . . Ortego, J. (2019). Modeling Arboviral Infection in Mice Lacking the Interferon Alpha/Beta Receptor. *Viruses, 11*(1). doi:10.3390/v11010035

Michalaki, C., Dean, C., & Johansson, C. (2022). The Use of Precision-Cut Lung Slices for Studying Innate Immunity to Viral Infections. *Curr Protoc, 2*(8), e505. doi:10.1002/cpz1.505

Molina-Torres, C. A., Flores-Castillo, O. N., Carranza-Torres, I. E., Guzmán-Delgado, N. E., Viveros-Valdez, E., Vera-Cabrera, L., . . . Carranza-Rosales, P. (2020). Ex vivo infection of murine precision-cut lung tissue slices with Mycobacterium abscessus: a model to study antimycobacterial agents. *Ann Clin Microbiol Antimicrob, 19*(1), 52. doi:10.1186/s12941-020-00399-3

Montel-Hagen, A., Sun, V., Casero, D., Tsai, S., Zampieri, A., Jackson, N., . . . Crooks, G. M. (2020). In Vitro Recapitulation of Murine Thymopoiesis from Single Hematopoietic Stem Cells. *Cell Rep, 33*(4), 108320. doi:10.1016/j.celrep.2020.108320

Moradali, M. F., Ghods, S., & Rehm, B. H. (2017). Lifestyle: A Paradigm for Adaptation, Survival, and Persistence. *Front Cell Infect Microbiol, 7*, 39. doi:10.3389/fcimb.2017.00039

Munyonho, F. T., Clark, R. D. E., Lin, D., Khatun, M. S., Pungan, D., Dai, G., & Kolls, J. K. (2024). Precision-cut lung slices as an. *mBio, 15*(1), e0146423. doi:10.1128/mbio.01464-23

Omar, T., Ziltener, P., Chamberlain, E., Cheng, Z., & Johnston, B. (2020). Mice Lacking γδ T Cells Exhibit Impaired Clearance of Pseudomonas aeruginosa Lung Infection and Excessive Production of Inflammatory Cytokines. *Infect Immun, 88*(6). doi:10.1128/IAI.00171-20

Patlin, B., Schwerdtfeger, L., & Tobet, S. (2023). Neuropeptide stimulation of physiological and immunological responses in precision-cut lung slices. *Physiol Rep, 11*(22), e15873. doi:10.14814/phy2.15873

Pechkovsky, D. V., Goldmann, T., Ludwig, C., Prasse, A., Vollmer, E., Müller-Quernheim, J., & Zissel, G. (2005). CCR2 and CXCR3 agonistic chemokines are differently expressed and regulated in human alveolar epithelial cells type II. *Respir Res, 6*(1), 75. doi:10.1186/1465-9921-6-75

Placke, M. E., & Fisher, G. L. (1987). Adult peripheral lung organ culture--a model for respiratory tract toxicology. *Toxicol Appl Pharmacol, 90*(2), 284-298. doi:10.1016/0041-008x(87)90336-x

Quigley, K. J., Reynolds, C. J., Goudet, A., Raynsford, E. J., Sergeant, R., Quigley, A., . . . Boyton, R. J. (2015). Chronic Infection by Mucoid Pseudomonas aeruginosa Associated with Dysregulation in T-Cell Immunity to Outer Membrane Porin F. *Am J Respir Crit Care Med, 191*(11), 1250-1264. doi:10.1164/rccm.201411-1995OC

Rosales Gerpe, M. C., van Vloten, J. P., Santry, L. A., de Jong, J., Mould, R. C., Pelin, A., . . . Wootton, S. K. (2018). Use of Precision-Cut Lung Slices as an. *Mol Ther Methods Clin Dev, 10*, 245-256. doi:10.1016/j.omtm.2018.07.010

Rosendahl Huber, S., van Beek, J., de Jonge, J., Luytjes, W., & van Baarle, D. (2014). T cell responses to viral infections - opportunities for Peptide vaccination. *Front Immunol, 5*, 171. doi:10.3389/fimmu.2014.00171

Roulová, N., Mot'ková, P., Brožková, I., & Pejchalová, M. (2022). Antibiotic resistance of Pseudomonas aeruginosa isolated from hospital wastewater in the Czech Republic. *J Water Health, 20*(4), 692-701. doi:10.2166/wh.2022.101

Salinas, F. M., Nebreda, A. D., Vázquez, L., Gentilini, M. V., Marini, V., Benedetti, M., . . . Bueno, C. A. (2020). Imiquimod suppresses respiratory syncytial virus (RSV) replication via PKA pathway and reduces RSV induced-inflammation and viral load in mice lungs. *Antiviral Res, 179*, 104817. doi:10.1016/j.antiviral.2020.104817

Sarathy, V. V., White, M., Li, L., Gorder, S. R., Pyles, R. B., Campbell, G. A., . . . Barrett, A. D. (2015). A lethal murine infection model for dengue virus 3 in AG129 mice deficient in type I and II interferon receptors leads to systemic disease. *J Virol, 89*(2), 1254-1266. doi:10.1128/JVI.01320-14

Schmitt, T. M., & Zúñiga-Pflücker, J. C. (2002). Induction of T cell development from hematopoietic progenitor cells by delta-like-1 in vitro. *Immunity, 17*(6), 749-756. doi:10.1016/s1074-7613(02)00474-0

Schraufnagel, D. E. (2020). The health effects of ultrafine particles. *Exp Mol Med, 52*(3), 311-317. doi:10.1038/s12276-020-0403-3

Schwerdtfeger, L. A., Nealon, N. J., Ryan, E. P., & Tobet, S. A. (2019). Human colon function ex vivo: Dependence on oxygen and sensitivity to antibiotic. *PLoS One, 14*(5), e0217170. doi:10.1371/journal.pone.0217170

Sewald, K., & Danov, O. (2022). Infection of Human Precision-Cut Lung Slices with the Influenza Virus. *Methods Mol Biol, 2506*, 119-134. doi:10.1007/978-1-0716-2364-0_9

Sheng, J. A., & Tobet, S. A. (2024). Maternal immune activation with toll-like receptor 7 agonist during mid-gestation alters juvenile and adult developmental milestones and behavior. *J Neuroendocrinol*, e13417. doi:10.1111/jne.13417

Shepherd, F. R., & McLaren, J. E. (2020). T Cell Immunity to Bacterial Pathogens: Mechanisms of Immune Control and Bacterial Evasion. *Int J Mol Sci, 21*(17). doi:10.3390/ijms21176144

Siddqui, G., Vishwakarma, P., Saxena, S., Kumar, V., Bajpai, S., Kumar, A., . . . Samal, S. (2024). Aged AG129 mice support the generation of highly virulent novel mouse-adapted DENV (1-4) viruses exhibiting neuropathogenesis and high lethality. *Virus Res, 341*, 199331. doi:10.1016/j.virusres.2024.199331

St Clair, L. A., Mills, S. A., Lian, E., Soma, P. S., Nag, A., Montgomery, C., . . . Perera, R. (2022). Acyl-Coa Thioesterases: A Rheostat That Controls Activated Fatty Acids Modulates Dengue Virus Serotype 2 Replication. *Viruses, 14*(2). doi:10.3390/v14020240

Stegmayr, J., Alsafadi, H. N., Langwiński, W., Niroomand, A., Lindstedt, S., Leigh, N. D., & Wagner, D. E. (2021). Isolation of high-yield and -quality RNA from human precision-cut lung slices for RNA-sequencing and computational integration with

larger patient cohorts. *Am J Physiol Lung Cell Mol Physiol, 320*(2), L232-L240. doi:10.1152/ajplung.00401.2020

Strunz, M., Simon, L. M., Ansari, M., Kathiriya, J. J., Angelidis, I., Mayr, C. H., . . . Schiller, H. B. (2020). Alveolar regeneration through a Krt8+ transitional stem cell state that persists in human lung fibrosis. *Nat Commun, 11*(1), 3559. doi:10.1038/s41467-020-17358-3

Thach, D. C., Kimura, T., & Griffin, D. E. (2000). Differences between C57BL/6 and BALB/cBy mice in mortality and virus replication after intranasal infection with neuroadapted Sindbis virus. *J Virol, 74*(13), 6156-6161. doi:10.1128/jvi.74.13.6156-6161.2000

The lungs at the frontlines of immunity. (2015). *Nat Immunol, 16*(1), 17. doi:10.1038/ni.3069

Tough, D. F., Sun, S., & Sprent, J. (1997). T cell stimulation in vivo by lipopolysaccharide (LPS). *J Exp Med, 185*(12), 2089-2094. doi:10.1084/jem.185.12.2089

Uddbäck, I., Cartwright, E. K., Schøller, A. S., Wein, A. N., Hayward, S. L., Lobby, J., . . . Christensen, J. P. (2021). Long-term maintenance of lung resident memory T cells is mediated by persistent antigen. *Mucosal Immunol, 14*(1), 92-99. doi:10.1038/s41385-020-0309-3

Ulmer, A. J., Flad, H., Rietschel, T., & Mattern, T. (2000). Induction of proliferation and cytokine production in human T lymphocytes by lipopolysaccharide (LPS). *Toxicology, 152*(1-3), 37-45. doi:10.1016/s0300-483x(00)00290-0

Vahedi, L., Jabarpoor-Bonyadi, M., Ghojazadeh, M., Vahedi, A., & Rafeey, M. (2016). Gender Differences in Clinical Presentations of Cystic Fibrosis Patients in Azeri Turkish Population. *Tuberc Respir Dis (Seoul), 79*(4), 267-273. doi:10.4046/trd.2016.79.4.267

Viana, F., O'Kane, C. M., & Schroeder, G. N. (2022). Precision-cut lung slices: A powerful ex vivo model to investigate respiratory infectious diseases. *Mol Microbiol, 117*(3), 578-588. doi:10.1111/mmi.14817

Vinod, N., Hwang, D., Azam, S. H., Van Swearingen, A. E. D., Wayne, E., Fussell, S. C., . . . Kabanov, A. V. (2020). High-capacity poly(2-oxazoline) formulation of TLR 7/8 agonist extends survival in a chemo-insensitive, metastatic model of lung adenocarcinoma. *Sci Adv, 6*(25), eaba5542. doi:10.1126/sciadv.aba5542

Wahl, A., De, C., Abad Fernandez, M., Lenarcic, E. M., Xu, Y., Cockrell, A. S., . . . Victor Garcia, J. (2019). Precision mouse models with expanded tropism for human pathogens. *Nat Biotechnol, 37*(10), 1163-1173. doi:10.1038/s41587-019-0225-9

Wang, A., Lee, M., Keller, A., Jian, S., Lowe, K., Finklea, J. D., & Jain, R. (2024). Sex differences in outcomes of people with cystic fibrosis treated with

elexacaftor/tezacaftor/ivacaftor. *J Cyst Fibros, 23*(1), 91-98. doi:10.1016/j.jcf.2023.05.009

Weiskopf, D., & Sette, A. (2014). T-cell immunity to infection with dengue virus in humans. *Front Immunol, 5*, 93. doi:10.3389/fimmu.2014.00093

World Health Organization. (2020, December 9). The top 10 causes of death. World Health Organization. https://www.who.int/news-room/fact-sheets/detail/the-top-10-causes-of-death#:~:text=Lower%20respiratory%20infections%20remained%20the,000%20fewer%20than%20in%202000.

World Health Organization. (2024, May 30). Dengue - global situation. World Health Organization. https://www.who.int/emergencies/disease-outbreak-news/item/2024-DON518

Wu, W., Huang, J., Duan, B., Traficante, D. C., Hong, H., Risech, M., . . . Priebe, G. P. (2012). Th17-stimulating protein vaccines confer protection against Pseudomonas aeruginosa pneumonia. *Am J Respir Crit Care Med, 186*(5), 420-427. doi:10.1164/rccm.201202-0182OC

Xu, H., Liew, L. N., Kuo, I. C., Huang, C. H., Goh, D. L., & Chua, K. Y. (2008). The modulatory effects of lipopolysaccharide-stimulated B cells on differential T-cell polarization. *Immunology, 125*(2), 218-228. doi:10.1111/j.1365-2567.2008.02832.x

Yunis, J., Short, K. R., & Yu, D. (2023). Severe respiratory viral infections: T-cell functions diverging from immunity to inflammation. *Trends Microbiol, 31*(6), 644-656. doi:10.1016/j.tim.2022.12.008

Zhang, X., Ali, M., Pantuck, M. A., Yang, X., Lin, C. R., Bahmed, K., . . . Tian, Y. (2023). CD8 T cell response and its released cytokine IFN-γ are necessary for lung alveolar epithelial repair during bacterial pneumonia. *Front Immunol, 14*, 1268078. doi:10.3389/fimmu.2023.1268078

Zhang, X., Wei, Z., Yong, T., Li, S., Bie, N., Li, J., . . . Gan, L. (2023). Cell microparticles loaded with tumor antigen and resiquimod reprogram tumor-associated macrophages and promote stem-like CD8. *Nat Commun, 14*(1), 5653. doi:10.1038/s41467-023-41438-9

Ziegler, U., Fischer, D., Eiden, M., Reuschel, M., Rinder, M., Müller, K., . . . Keller, M. (2019). Sindbis virus- a wild bird associated zoonotic arbovirus circulates in Germany. *Vet Microbiol, 239*, 108453. doi:10.1016/j.vetmic.2019.108453

Zimmerman, L. M., Clairardin, S. G., Paitz, R. T., Hicke, J. W., LaMagdeleine, K. A., Vogel, L. A., & Bowden, R. M. (2013). Humoral immune responses are maintained with age in a long-lived ectotherm, the red-eared slider turtle. *J Exp Biol, 216*(Pt 4), 633-640. doi:10.1242/jeb.078832

Zompi, S., Santich, B. H., Beatty, P. R., & Harris, E. (2012). Protection from secondary dengue virus infection in a mouse model reveals the role of serotype cross-reactive B and T cells. *J Immunol, 188*(1), 404-416. doi:10.4049/jimmunol.1102124